Walnut Shells and Eucalyptus Bark as Green Alternatives to Chemical Coagulants in Water Treatment

Isabella Kaminski Aires

Dissertation submitted to
Escola Superior de Tecnologia e Gestão - Instituto Politécnico de Bragança
to obtain
Master’s degree in Chemical Engineering
under de Double Degree program with the Federal University of Technology – Paraná

Supervisor:
Prof. Ramiro José Espinheira Martins
Co-supervisor:
Prof. Juliana Martins Teixeira de Abreu Pietrobelli

May 2026

Acknowledgements

I would like to begin by thanking my parents, João Paulo Aires and Simone Bello Kaminski Aires, my greatest examples of kind people and outstanding professionals, for all their support throughout my undergraduate studies, in my personal and professional choices, during my good days when our phone calls were calm and joyful, and during the difficult days when every conversation became an emotional outpouring and they always offered me comfort and encouragement to persevere. Above all, I would like to thank you for giving me the incredible opportunity to come to Portugal and participate in the double degree program. Even from afar, I thought about you every single day. I love you both very much.

I would also like to thank my partner, Murilo Gomes Marçal, who, despite the emotional difficulties, was the first person to encourage me to come here. Even with the long distance and time zone differences, he always supported me through every moment, during the good days when everything was going well and during the hard days when homesickness felt stronger than the desire to continue. Thank you for all your support; without you, I would not have been able to complete this journey.

To the rest of my family, I am deeply grateful for your support and for doing your best to remain present in my daily life, as well as to my partner's family and friends in Brazil. All of you made a difference in my routine and constantly reminded me how much I missed you whenever you gathered.

I would also like to thank my colleague Juliana Akemy Inamine Vieira, whom I have known for many years and who agreed to join the double degree program and accompany me on this journey. Every day was lighter by your side, and I am grateful for your support and companionship.

Finally, I would like to express my sincere gratitude to Professors Ramiro José Espinheira Martins and Juliana Martins Teixeira de Abreu Pietrobelli for their guidance and constant availability to assist us whenever needed throughout the development of this work. I would also like to thank Eng. Maria João Afonso, laboratory technician at LPQ, who welcomed us from the very first day and was always there whenever we needed help.

Abstract

Water resource management has become a major technical and environmental challenge of the 21st century, largely driven by the intensification of industrial activities and the resulting generation of increasingly complex wastewater. Conventional coagulation–flocculation processes, widely used in wastewater treatment plants, mainly rely on inorganic chemical coagulants, such as aluminum and iron salts. Although effective, these chemicals have notable environmental and operational limitations. In response to these challenges, growing attention has been given to developing of more sustainable alternatives aligned with the principles of green chemistry. In this context, this study investigated the potential of natural coagulants derived from walnut shells (Juglans regia) and eucalyptus bark (Eucalyptus spp.) as environmentally friendly alternatives to conventional chemical coagulants. These lignocellulosic materials are rich in tannins, polyphenols, and other bioactive functional groups that promote coagulation primarily through charge neutralization and polymer bridging mechanisms. Unlike many approaches reported in the literature, which rely on raw powders or chemically activated adsorbents, this study employed saline-assisted liquid extracts, providing a milder, more more sustainable extraction route. The results demonstrated that eucalyptus bark exhibited superior turbidity removal performance, reaching 91%, while walnut shell achieved a maximum of 80%. For color removal using methylene blue, both biomaterials showed comparable performance, with maximum efficiencies of 48% for eucalyptus bark and 47% for walnut bark. A comparative analysis with the literature confirmed that the observed efficiencies were lower than those reported for chemically activated or highly optimized systems; however, they remained relevant within the context of green, low-cost, and minimally processed treatment strategies. This study advances environmentally friendly water treatment technologies by systematically comparing two forest residues under mild extraction conditions, supporting their potential application as scalable alternatives to conventional coagulants.

Keywords: Biocoagulants, Coagulation process, Eucalyptus bark, Sustainable water treatment, Walnut shells.

Resumo

A gestão dos recursos hídricos tornou-se um dos principais desafios técnicos e ambientais do século XXI, impulsionado sobretudo pela intensificação das actividades industriais e pela consequente geração de águas residuais cada vez mais complexas. Os processos convencionais de coagulação–floculação, amplamente utilizados em estações de tratamento de águas residuais, dependem principalmente de coagulantes químicos inorgânicos, como sais de alumínio e ferro. Embora eficazes, estes produtos químicos apresentam limitações ambientais e operacionais significativas. Em resposta a estes desafios, tem crescido o interesse no desenvolvimento de alternativas mais sustentáveis e alinhadas com os princípios da química verde. Neste contexto, o presente estudo investigou o potencial de coagulantes naturais derivados de cascas de noz (Juglans regia) e casca de eucalipto (Eucalyptus spp.) como alternativas ambientalmente sustentáveis aos coagulantes químicos convencionais. Estes materiais lignocelulósicos são ricos em taninos, polifenóis e outros grupos funcionais bioactivos que promovem a coagulação principalmente através de mecanismos de neutralização de carga e formação de pontes poliméricas. Ao contrário de muitas abordagens descritas na literatura, que utilizam pós brutos ou adsorventes quimicamente activados, este estudo empregou extractos líquidos assistidos por solução salina, proporcionando uma rota de extracção mais suave e sustentável. Os resultados demonstraram que a casca de eucalipto apresentou desempenho superior na remoção de turbidez, atingindo 91%, enquanto a casca de noz alcançou um máximo de 80%. Para a remoção de cor utilizando azul de metileno, ambos os biomateriais apresentaram desempenho semelhante, com eficiências máximas de 48% para a casca de eucalipto e 47% para a casca de noz. Uma análise comparativa com a literatura confirmou que as eficiências observadas foram inferiores às reportadas para sistemas quimicamente activados ou altamente optimizados; contudo, os resultados mantiveram-se relevantes no contexto de estratégias de tratamento verdes, de baixo custo e minimamente processadas. Este estudo contribui para o avanço de tecnologias ambientalmente sustentáveis para o tratamento de água ao comparar sistematicamente dois resíduos florestais sob condições suaves de extracção, reforçando o seu potencial de aplicação como alternativas escaláveis aos coagulantes convencionais.

Palavras-chave: Biocoagulantes, Casca de eucalipto, Cascas de noz, Processo de coagulação, Tratamento sustentável da água.

Index

List of Figures

List of Tables

List of Abbreviations

ANOVA	Analysis of Variance
BBD	Box–Behnken Design
RSM	Response Surface Methodology
WWTPs	Wastewater Treatment Plants

1. Introduction

The rapid growth of industrial and urban activities has resulted in a marked increase in the volume of wastewater containing high levels of turbidity, color, and suspended solids, which creates significant challenges for wastewater treatment plants (WWTPs). Coagulation–flocculation is a key step in the removal of colloidal particles and colored substances. However, the continued reliance on conventional inorganic coagulants, such as aluminum and iron salts, raises important environmental, operational, and economic concerns regarding their use. These include excessive sludge generation, pH fluctuations, the presence of residual metals in treated effluents, and dependence on non-renewable chemical reagents.

In response to these challenges, biocoagulants obtained from renewable biological sources particularly those derived from lignocellulosic agro-industrial subproducts, have gained increasing attention. The use of these materials is consistent with the principles of green chemistry and the circular economy, as they promote waste valorization while reducing the environmental impact of the treatment processes. Among the various sources investigated, walnut shells (*Juglans regia*), as shown in Figure 1, and eucalyptus bark (*Eucalyptus spp.*), as shown in Figure 2, are abundant lignocellulosic residues rich in tannins and polyphenolic compounds.

Figure 1. Walnut shells (Juglans regia)

Figure 2. Eucalyptus bark (Eucalyptus spp.)

These constituents contain a high density of reactive functional groups, such as hydroxyl and carboxyl moieties, which promote effective interactions with suspended particles in the aqueous systems. Consequently, their coagulation performance is primarily associated with mechanisms including charge neutralization, which reduces the electrostatic repulsion between colloids, and polymer bridging, whereby macromolecular structures link multiple particles and enhance floc formation.

Although research on natural coagulants has grown significantly in recent years, important knowledge gaps remain. In particular, the influence of different extraction media on the performance of walnut shell- and eucalyptus bark-based biocoagulants is not yet fully understood, especially when saline (NaCl, KCl) or alkaline (NaOH) extraction methods are applied. Current studies on lignocellulosic bioproducts have predominantly focused on their application as adsorbents, with limited attention given to their coagulation performance. Furthermore, many published studies on natural coagulants have relied on synthetic model water to evaluate coagulation efficiency under controlled conditions. Although this approach enables a systematic investigation of coagulation mechanisms, further research is necessary to better understand how extraction strategies affect both performance and operational behavior. Therefore, evaluating biocoagulant performance in controlled synthetic systems, such as kaolin suspensions, provides valuable insights into their mechanisms of action and supports the optimization of their application in water and wastewater treatments.

.

The pH is another critical aspect, as it strongly influences coagulation efficiency by affecting the ionization of functional groups, particle surface charge, and floc formation. A systematic assessment of turbidity removal across different pH conditions is necessary to identify the optimal operating range for each of the biocoagulants. Beyond turbidity, color removal is also a key performance indicator, particularly in wastewater containing dyes and other organic chromophores. In this context, methylene blue is commonly used as a model compound to evaluate the removal of cationic dyes and gain insights into the interactions between biocoagulants and dissolved organic pollutants.

Against this background, the present study aims to provide experimental evidence on the performance, operating conditions, and practical applicability of biocoagulants derived from walnut shells and eucalyptus bark, extracted using different chemical media and at different coagulant doses. This study aims to contribute to the development of more sustainable and effective alternatives for water and wastewater treatment.

1.1 Objectives

1.1 General Objective

The main objective of this dissertation is to evaluate the coagulation–flocculation performance of biocoagulants derived from walnut shells (*Juglans regia*) and eucalyptus bark (*Eucalyptus* spp.) extracted using different chemical agents, with an emphasis on turbidity and color removal in synthetic water to simulate industrial wastewater.

1.2 Specific Objectives

- To extract biocoagulants from walnut shells and eucalyptus bark using different chemical agents (NaCl, KCl, and NaOH) and investigate the influence of the extraction medium on their efficiency.
- To assess turbidity removal in synthetic water prepared with kaolin suspensions under controlled laboratory conditions.
- To study the effect of pH on coagulation performance and to determine the optimal pH range for each biocoagulant and extraction method.
- To evaluate color removal efficiency using methylene blue as a basic textile dye.

- To correlate turbidity and color removal results with pH conditions in order to elucidate the underlying coagulation mechanism.
- To compare the performance of walnut shell and eucalyptus bark biocoagulants to assess their potential as sustainable alternatives to conventional chemical coagulants.

2. State of The Art

The expansion of industrial and urban activities in recent decades has led to a marked increase in the generation of complex wastewater streams containing high levels of suspended solids, turbidity, synthetic dyes, heavy metals, and persistent organic compounds. Effluents produced by sectors such as textile manufacturing, pulp and paper, mining, petroleum refining, and food processing often present characteristics that challenge conventional treatment technologies, particularly because of their intense color and high colloidal particle content (Carneiro et al., 2010; Khan et al., 2023). When inadequately treated wastewater is discharged into surface or groundwater bodies, it can cause serious environmental degradation, pose risks to human health, and compromise the availability of freshwater resources for domestic, agricultural, and industrial use (Vilela et al., 2018; Menezes et al., 2025). These concerns highlight the urgent need for treatment strategies that are not only effective but also environmentally sustainable and cost effective.

Coagulation–flocculation remains one of the most widely applied processes in municipal and industrial wastewater treatment, as it enables the destabilization and removal of colloidal particles from wastewater. Conventional treatment systems predominantly rely on inorganic chemical coagulants, such as aluminum sulfate, ferric chloride, and polyaluminum chloride, owing to their low cost, widespread availability, and high removal efficiency (Abdo et al., 2020; Lim et al., 2021; Lima et al., 2020; Ndayako et al., 2023). These coagulants mainly act through mechanisms such as charge neutralization, sweep coagulation, and compression of the electrical double layer, which promote particle aggregation and sedimentation. However, the use of chemical coagulants is associated with several environmental and operational limitations.

The generation of large volumes of metal-rich sludge increases the treatment costs related to dewatering, handling, and disposal (Kumar et al., 2024). In addition, residual aluminum or iron may remain in the treated effluent, raising concerns about its potential impact on human health and long-term environmental effects (Uwanta et al., 2022; Benalia et al., 2024). Other limitations include pH instability, particularly in systems using aluminum-based coagulants, and limited effectiveness in removing emerging contaminants such as pharmaceuticals, endocrine disruptors, and persistent dyes (Vilela et al., 2018; Khan et al., 2023; Husen et al., 2024). These challenges have motivated increasing interest in alternative coagulation strategies that combine high efficiency with improved environmental performance.

In this context, natural coagulants, commonly referred to as biocoagulants, have emerged as promising alternatives to conventional chemical coagulants. Biocoagulants derived from renewable biological sources mainly consist of complex organic polymers, such as proteins, polysaccharides, and polyphenolic compounds, particularly tannins, which contain functional groups capable of interacting with suspended and colloidal particles (Benalia et al., 2024; Husen et al., 2024). Unlike metallic salts, whose coagulation performance depends largely on electrostatic compression, biocoagulants predominantly act through charge neutralization and polymer bridging. These interactions often result in the formation of larger and denser flocs, improved settling behavior, and reduced sludge production, while avoiding the introduction of residual metals into treated water (Benalia et al., 2024; Choy et al., 2014).

A wide range of biological materials has been investigated as potential biocoagulants. Notable examples include *Moringa oleifera* seeds, which are rich in cationic proteins, cationic starches derived from tubers and cereals, and plant seed extracts such as flaxseed and watermelon. These materials have demonstrated moderate to high efficiencies in turbidity and color removal in both laboratory and pilot-scale studies (Abdo et al., 2020; Ndayako et al., 2023; Husen et al., 2024). In addition, tannin-rich tree barks, *Jatropha* extracts, and polysaccharides obtained from algae and other plant residues show considerable potential as biocoagulants. In addition to their treatment performance, these materials offer the added benefit of being derived from renewable and often underutilized biomass, contributing to waste valorization and circular economy strategies (Benalia et al., 2024; Al-Hanaktah   Pérez, 2026).

Among the most promising lignocellulosic sources, walnut shells (*Juglans regia*) and eucalyptus bark (*Eucalyptus* spp.) have attracted considerable attention. Walnut shells are an abundant agro-industrial residue characterized by a porous structure and high lignin and cellulose content, which confer significant physicochemical stability to the material. Their high tannin content supports coagulation through charge neutralization and polymer bridging, enabling efficient turbidity removal over a wide pH range (Jahanban-Esfahlan et al., 2020; Zedan et al., 2022; Zourif et al., 2024; Tomasi et al., 2025). Recent studies have reported turbidity removal efficiencies ranging from 85% to 98%, often with minimal changes in total organic carbon and without the need for significant pH adjustment, in contrast to aluminum-based coagulants (Zedan et al., 2022). In addition to their role as biocoagulants, walnut shells have been explored as biosorbents for heavy metals, highlighting their multifunctional potential in wastewater treatment applications (Nujkic et al., 2023).

Eucalyptus bark, a major byproduct of the forestry industry, is another promising biocoagulant precursor owing to its high condensed tannin and polyphenol content. These compounds impart strong coagulating properties, which can be further enhanced through chemical modification processes such as cationization or the Mannich reaction. Such modifications allow eucalyptus-derived materials to behave as high-performance polyelectrolytes, with efficiencies comparable to those of synthetic polymers (Klumb Faria, 2013; Grenda et al., 2019; Tomasi et al., 2023). Studies have shown that eucalyptus bark biocoagulants are particularly effective in color removal and reducing dissolved organic matter while maintaining near-neutral pH conditions during treatment.

From a circular economy perspective, the selection of walnut shells and eucalyptus bark is particularly strategic in this study. The circular economy model promotes the transition from a linear “take–make–dispose” system toward regenerative production systems in which residues are reintegrated into value chains as secondary raw materials (Geissdoerfer et al., 2017; Kirchherr et al., 2017). In this framework, the transformation of agro-industrial and forestry residues into functional materials for water treatment represents a high-value valorization pathway that simultaneously addresses waste management challenges and the increasing demand for sustainable and low-impact technologies.

Walnut shells are an unavoidable byproduct of walnut processing, representing approximately 40–60% of the total fruit mass (Jahanban-Esfahlan et al., 2020; Acoglu et al., 2025). Global walnut production has exceeded 3 million tonnes annually in recent years, with major producers including China, the United States, Iran, and Turkey (World Population Review, 2026). Considering the proportion of shell mass, this corresponds to an estimated generation of more than 2 million tonnes of walnut shell residues annually worldwide. Chemically, walnut shells are rich in lignin (~50%), cellulose (~25%), hemicellulose, and polyphenolic compounds, which confer structural stability and reactive functional groups suitable for environmental applications (Acoglu et al., 2025).

The conventional large-scale uses of walnut shells include abrasive blasting media, fillers in composite materials, activated carbon precursors, and direct combustion for energy recovery (Jahanban-Esfahlan et al., 2020). Such applications do not fully exploit their intrinsic tannin and phenolic functionalities, which are directly relevant for coagulation–flocculation mechanisms and natural coagulation and adsorption applications.

Similarly, eucalyptus bark is a large-scale byproduct of the forestry and pulp industries. Eucalyptus plantations occupy more than 20 million hectares globally, with major production concentrated in Brazil, Portugal, Spain, China, and Australia (FAO, 2020). During industrial wood processing for pulp and paper production, bark is mechanically removed and may represent 7–20% of the total tree biomass (Miranda et al., 2013; Chemetova et al., 2018), resulting in the generation of millions of tons of bark annually. Although a significant fraction is currently used for biomass energy, recent studies have emphasized the environmental and economic advantages of extracting tannins and polyphenols from bark residues for application in water treatment systems (Simões et al., 2025). The tannin content of eucalyptus bark may exceed 10%, depending on the species and extraction conditions, providing strong chemical functionality for coagulation and flocculation processes (Grenda et al., 2021; Tomasi et al., 2023).

The large-scale availability and demonstrated technological versatility of these biomass streams reinforce their feasibility as sustainable raw materials for biocoagulant production. Importantly, walnut shells and eucalyptus bark do not require additional land use, irrigation, or agricultural inputs, as they are unavoidable residues in established agro-industrial and forestry supply chains (Geissdoerfer et al., 2017). Their valorization aligns with key sustainability principles, including resource efficiency, waste minimization, reduction of greenhouse gas emissions associated with combustion, and the substitution of non-renewable chemical coagulants (Kirchherr et al., 2017; Benalia et al., 2024).

Moreover, integrating these residues into wastewater treatment technologies promotes cross-sectoral industrial symbiosis, linking the agriculture, forestry, and environmental engineering sectors (Al-Hanaktah Pérez, 2026). Such integration enhances material circularity, diversifies revenue streams for primary industries, and may contribute to cost reduction in treatment systems by providing locally available, renewable, and potentially lower-cost alternatives to conventional chemical coagulants.

Therefore, beyond their demonstrated performance in adsorption and emerging pollutant removal, walnut shells and eucalyptus bark represent strategically abundant, renewable, and underutilized biomass resources. Their conversion into biocoagulants constitutes a logical next step in the evolution of lignocellulosic residue valorization, embodying a practical implementation of circular economy principles and transforming high-volume agroforestry residues into high-performance materials for sustainable water and wastewater treatment applications.

The performance of lignocellulosic biocoagulants is strongly influenced by the extraction method, which determines the availability and composition of active compounds, such as tannins, proteins, and polysaccharides. Saline extraction using NaCl or KCl favors protein solubilization while preserving the polymer structure. In contrast, alkaline extraction with NaOH enhances the release of polyphenolic compounds but may alter the polymer properties and pH sensitivity (Husen et al., 2024; Tomasi et al., 2025). Consequently, optimizing the extraction conditions is a key factor in maximizing coagulation efficiency, improving color removal, and identifying suitable operational pH ranges.

From technological and market perspectives, biocoagulants derived from agro-industrial residues offer several advantages, including reduced sludge generation, lower environmental impact, potential for decentralized or on-site production, and valorization of low-value biomass. These attributes align with global trends toward sustainable water treatment solutions and the replacement of nonrenewable chemical inputs. In recent years, experimental investigations and applied studies have demonstrated growing interest in biocoagulants for applications such as municipal wastewater treatment, industrial effluent clarification and dye removal.

Despite the promising results reported in the literature, important research gaps remain. Comparative studies examining the influence of different extraction methods on biocoagulant performance are limited, particularly under real wastewater conditions. A systematic evaluation of turbidity and color removal in both synthetic and real effluents is also required, as well as the identification of optimal pH conditions for maximum efficiency. Addressing these gaps is essential to confirm the technical feasibility, operational reliability, and practical applicability of biocoagulants as sustainable alternatives to conventional chemical coagulants.

In light of these considerations, the present study aimed to address existing knowledge gaps by evaluating biocoagulants derived from walnut shells and eucalyptus bark, extracted using NaCl, KCl, and NaOH solutions. Their performance was assessed in synthetic kaolin suspensions, with emphasis on turbidity, color removal and pH optimization. This study contributes to the advancement of sustainable and environmentally responsible solutions for water and wastewater treatment, supporting the transition toward renewable, high-performance biocoagulants within a circular economy framework.

3. Methodology

The methodological framework adopted in this study was developed to enable a comprehensive evaluation of the coagulation performance of walnut shells (*Juglans regia*) and eucalyptus bark (*Eucalyptus* spp.). The experimental work encompassed the extraction of the biocoagulants, synthetic water preparation, followed by their application in synthetic wastewater jar tests and color removal experiments. The effectiveness of the coagulation–flocculation process was assessed primarily through turbidity and color removal, and the optimal pH conditions and coagulant doses were investigated.

3.1 Biocoagulant Extraction

Biocoagulant extraction was carried out using three different chemical agents, NaCl and KCl for the saline extractions and NaOH for the alkaline extractions, to explore how the chemical agents influence the recovery of active compounds responsible for coagulation performance. These compounds include proteins, polysaccharides, and polyphenolic constituents that contribute to particle destabilization and floc formation.

Prior to the extraction procedures, the walnut shells were separated from the pulp and broken into smaller pieces, while the eucalyptus bark was also fragmented into smaller pieces to facilitate the drying and milling processes, and then cleaned with distilled water. Both biomasses were dried in an oven at 60 °C for 24 h. After drying, the materials were removed from the oven and milled, as illustrated in Figures 3 and 4, to increase the surface area available for extraction.

Subsequently, the milled materials were returned to the oven and dried again at 60 °C for an additional 24 h to remove any remaining moisture residues. After drying, the ground biomass was sieved to obtain uniform particle sizes. The walnut shell powder achieved a particle size range of 106–160 µm, while the eucalyptus bark reached a finer granulometry below 53 µm.

Figure 3. Milled walnut shells (Juglans regia)

Figure 4. Milled eucalyptus bark (Eucalyptus spp.)

To determine the most suitable compounds for the extraction process for each type of biomass, preliminary tests were carried out to evaluate their respective concentrations for biocoagulant extraction. For the extraction, a proportion of 5 g of biomass was added to 100 mL of NaCl, KCl, or NaOH, and the initial concentrations of each compound were 1.0 M NaCl, 1.0 M KCl, and 0.05 M NaOH. The mixtures were then subjected to orbital agitation at 160 rpm at room temperature for 24 h.

After the extraction process, the solutions were filtered using a vacuum pump to separate the shells from the solution (insoluble material) and obtain the liquid extract for use in the tests. The extracts were then stored in containers, as shown in Figures 5 and 6, and were kept refrigerated at 4 °C.

Figure 5. Walnut shells extracts

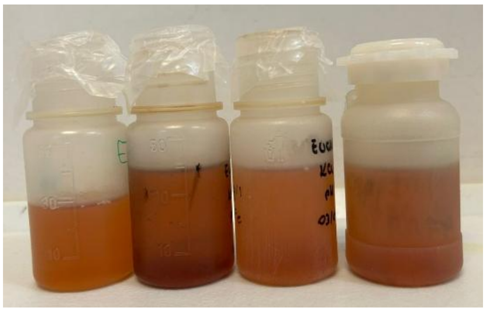

Figure 6. Eucalyptus bark extracts

3.2 Synthetic Wastewater Preparation

The coagulation performance was evaluated under controlled laboratory conditions using synthetic turbid water prepared with a kaolin suspension. This method provides consistent and reproducible experimental conditions for assessing the effectiveness of biocoagulants. The synthetic solution was prepared by diluting 5 g of kaolin powder in 1000 mL of distilled water to simulate highly turbid industrial wastewater conditions.

As illustrated in Figure 7, the kaolin suspension was prepared by adding kaolin powder to distilled water under continuous slow agitation at 30 rpm for 2 h to ensure proper particle dispersion. Subsequently, the suspension was allowed to rest for 24 h to promote complete kaolin hydration before use in the coagulation–flocculation experiments.

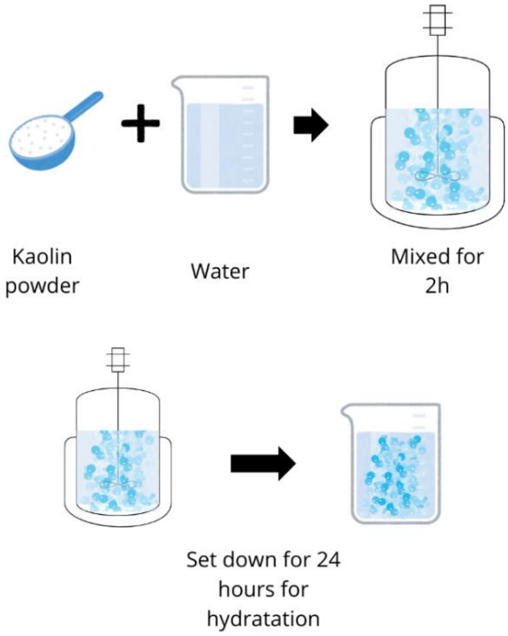

Figure 7. Synthetic water preparation.

After the resting period, the desired water turbidity was adjusted for the jar test experiments. Because the stock kaolin suspension presented high turbidity, it was diluted 15-fold to obtain a more suitable turbidity level for the experiments.

3.3 Preparation of Methylene Blue Stock Solution

The methylene blue stock solution used as a basic textile dye to simulate colored water was prepared by dissolving 1 g of methylene blue dye in 1 L of distilled water and stored for preliminary analyses. Subsequently, a calibration curve was established, as shown in Figure 8, using dilutions of the stock solution ranging from 0 to 10 mg L^{-1} of methylene blue. This calibration curve was used to determine the amount of dye removed from the solution after the addition of the natural coagulants during treatment.

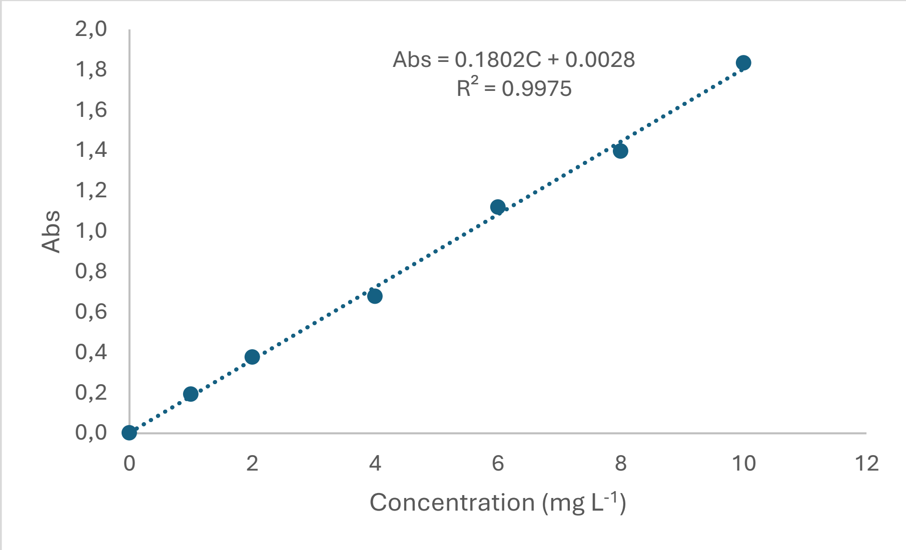

Figure 8. A methylene blue calibration curve ranging from 0 – 10 mg L^{-1}.

3.4 Coagulation-Flocculation Jar Tests

The coagulation performance was evaluated through standard jar test experiments. For each biocoagulant extract, the optimal coagulant dosage range for turbidity removal was investigated, as well as the most suitable operating pH under near-neutral conditions. Turbidity removal efficiency was quantified using a calibrated turbidimeter (VWR TIR210, VWR International, Germany) by measuring the initial turbidity (T_0) and the final turbidity (T_f) after the predetermined settling period. The turbidity removal efficiency was calculated using Equation 1.

$$Turbidity\ Removal\ (\%) = \frac{T_0 - T_f}{T_0} \tag{1}$$

The coagulation–flocculation performance of biocoagulants is associated with several physicochemical mechanisms, including electrostatic interactions, particle adsorption, charge neutralization, interparticle bridging, and electrical double-layer compression. These mechanisms contribute to the destabilization of suspended colloidal matter and favor the formation of larger aggregate. In natural biomass-derived coagulants, the presence of reactive functional groups enhances interactions with contaminants dispersed in water, thereby improving floc development and separation efficiency (Mohammad Ali et al., 2024).

Through these interactions, larger and denser flocs are formed and progressively sediment due to gravitational forces. As illustrated in Figure 9, the action of the biocoagulant promoted particle agglomeration and settling at the bottom of the beaker, resulting in a turbidity reduction in the treated water.

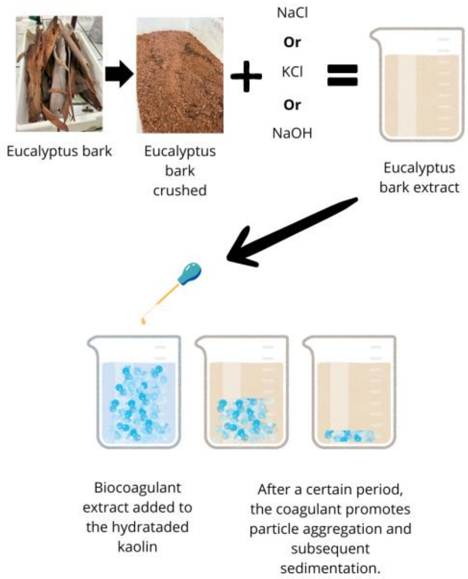

Figure 9. Effect of biocoagulant on synthetic water.

Jar test (Paralab - Equipamentos industriais de Laboratório, S.A., Portugal) experiments, as shown in Figure 10, were performed to evaluate the coagulation performance of each biocoagulant extract at different pH values and coagulant doses of 0.5, 1.0, and 1.5 mL for every 100 mL of synthetic water.

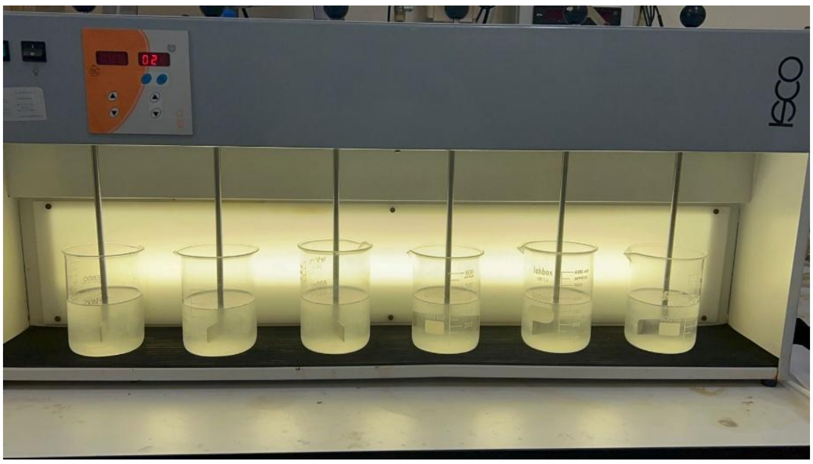

Figure 10. Jar Test experiments.

This phase enabled the identification of preliminary optimal operational conditions, evaluation of the influence of extraction methods on coagulation efficiency, determination of ideal pH ranges for each extracted coagulant, and comparison of turbidity removal performance. These experiments also allowed the identification of extracts with higher turbidity removal efficiencies under controlled conditions.

In this context, Mohammad Ali et al. (2024) emphasized that the performance of biomass-based natural coagulants is highly dependent on precise dosage control, which is considered one of the most critical operational parameters in coagulation processes. According to the authors, the effectiveness of turbidity removal is strongly influenced by the amount of extract applied, since an optimal dosage exists at which maximum coagulation efficiency is achieved. Below this optimum, underdosing results in insufficient neutralization of the particle surface charges, leading to poor floc formation and reduced turbidity removal. Overdosing can cause particle restabilization due to charge reversal or saturation of active sites, thereby decreasing treatment efficiency. Therefore, accurate dosage optimization is essential to ensure both high coagulation performance and process stability, while also contributing to reduced operational costs and improved sustainability of the treatment system (Mohammad Ali et al., 2024).

3.5 Color Removal Experiments

Color removal experiments were conducted using a spectrophotometer (Jasco, V-530, UV/VIS Spectrophotometer, Tokyo, Japan) during the same experimental period using methylene blue that had been prepared previously. These tests aimed to assess the capacity of biocoagulants to remove dissolved organic compounds and colored pollutants under the same jar test conditions used for turbidity assessment.

3.6 Experimental Optimization and Statistical Design

A systematic optimization of the extraction and coagulation conditions was carried out using statistical experimental design and modeling approaches. Initially, the experimental strategy was based on Response Surface Methodology (RSM) employing the Box–Behnken Design (BBD) to evaluate the influence of operational variables on the performance of walnut shell and eucalyptus bark based biocoagulants. The Box–Behnken

Design was selected due to its high statistical efficiency and its ability to generate reliable quadratic models with a reduced number of experimental runs compared with the conventional full factorial design (3^3).

BBD is a fundamental statistical tool for investigating complex relationships among multiple variables while minimizing the number of required experiments. In scientific and industrial studies, evaluating all possible combinations of factors can be impractical because of limitations associated with time, operational costs, and reagent consumption. Therefore, the BBD provides an efficient and systematic approach for exploring the response surface while maintaining experimental reliability and statistical robustness (Semassel et al., 2025).

The application of BBD presents important advantages for coagulation–flocculation studies, particularly because of the reduction in experimental runs, reagent consumption, and overall processing time required. In addition, unlike conventional factorial designs, the BBD avoids experimental points that are located at the extreme corners of the design space. This characteristic is particularly important for systems involving natural bioactive compounds, as excessively severe conditions may lead to the degradation of functional compounds or operational instability during the coagulation process. Instead, the BBD distributes the experimental runs at the midpoints of the edges and at the central points of the experimental domain, providing greater process stability and safer operational conditions.

Furthermore, the BBD enables the development of second-order polynomial models through regression analysis, allowing the quantitative evaluation of the relationships between independent and response variables. This approach provides valuable information regarding the individual effects of factors, interaction effects, and curvature responses, contributing to a deeper understanding of the complexity of the systems under study. In addition, BBD is highly effective in identifying optimal operational conditions that can maximize desired responses (Semassel et al., 2025).

In this study, the effects of extraction time (X_1) of 12, 24, and 36 h, coagulation pH, and extraction agent concentration were evaluated. For the walnut shell biocoagulants, pH (X_2) values of 6, 7, and 8 and NaCl concentrations (X_3) of 0.5, 1.0, and 1.5 M were evaluated, as shown in Table 1. For eucalyptus bark biocoagulants, coagulation pH values of 5, 6, and 7 and KCl concentrations of 0.5, 1.0, and 1.5 M were investigated (Table 2). The factor levels were coded as −1, 0, and +1 to facilitate statistical analysis and predictive model development.

Table 1. Coded factor table for walnut shells.

Factor	Symbol	(-1)	(0)	(+1)
Extraction time (h)	X_1	12	24	36
pH	X_2	6	7	8
NaCl conc.(M)	X_3	0.5	1.0	1.5

Table 2. Coded factor table for eucalyptus bark.

Factor	Symbol	(-1)	(0)	(+1)
Extraction time (h)	X_1	12	24	36
pH	X_2	5	6	7
KCl conc. (M)	X_3	0.5	1.0	1.5

The experimental design will include 17 runs for each biocoagulant, covering the combinations of the evaluated factors and five replicates at the central point. These central point repetitions were used to estimate the experimental error, assess the reproducibility, and detect curvature effects within the system. The treatment efficiency was primarily evaluated through turbidity removal using kaolin-based synthetic water as a model of industrial wastewater, and then it will be evaluated by the color removal of methylene blue.

The obtained results were analyzed using Analysis of Variance (ANOVA) and Response Surface Methodology (RSM). The integration of these statistical tools will contribute to the development of more efficient, sustainable, and economically viable water treatment processes using lignocellulosic biocoagulants.

3.6.1 Application of Response Surface Methodology and Box–Behnken Design

The extraction and coagulation conditions for walnut shell and eucalyptus bark biocoagulants were optimized using Response Surface Methodology (RSM) associated with Box–Behnken Design (BBD).

Statistical analysis was performed using Minitab software through quadratic regression modeling and Analysis of Variance (ANOVA). RSM was applied to generate predictive mathematical models and to identify the optimal extraction and coagulation conditions for each biocoagulant system.

$$Y = \beta_0 + \sum \beta_i X_i + \sum \beta_{ii} X_i^2 + \sum \beta_{ij} X_i X_j \qquad (2)$$

where:

- (Y) represents the predicted response variable;
- (β_0) is the intercept coefficient;
- (β_i) represents the linear coefficients;
- (β_{ii}) corresponds to the quadratic coefficients;
- (β_{ij}) represents the interaction coefficients between variables;
- (X_i) and (X_j) are the coded independent variables.

ANOVA was employed to evaluate the statistical significance of the developed models, as well as the individual and interaction effects of the studied factors using statistical parameters, such as F-values and p-values. The integration of RSM and ANOVA provided a comprehensive understanding of system behavior and contributed to the development of more efficient, sustainable, and economically viable water treatment processes using biocoagulants.

4. Results and Discussion

4.1 Preliminary Experiments

Preliminary experiments were performed to define the extraction conditions and operational parameters used in the BBD. Different extraction media and pH conditions were initially evaluated to identify the most suitable conditions for turbidity and color removal.

For turbidity removal, the results indicated that the optimum coagulation performance was achieved within a pH range of 4–6, likewise, the evaluation of color removal showed that the optimum performance also occurred within the same pH range. Therefore, pH 5 was selected as a fixed operating condition for all coagulation experiments performed in the BBD.

Regarding the extraction media, NaCl and KCl extracts exhibited the highest turbidity removal efficiencies for walnut shell and eucalyptus bark, respectively, and were therefore selected for optimization by the Box–Behnken Design. For color removal, eucalyptus bark extracts achieved the highest efficiencies when NaOH and KCl were used as extraction media, whereas NaOH and NaCl provided the best performance for walnut shell extracts. These preliminary results enabled the comparison of different extraction methods and the selection of the most effective extraction media for each biomass.

4.2 Walnut Shell Biocoagulant

4.2.1 General Turbidity Removal Performance

The results for the walnut-shell biocoagulant (Table 3) demonstrate excellent turbidity removal under all evaluated operational conditions, as shown in Figure 11. The experimental results revealed that the coagulation efficiency was strongly influenced by the extraction time, coagulation pH, NaCl concentration, and coagulant dosage.

Table 3. Walnut shells results for turbidity and color removal.

Sample	Time (h) [X_1]	pH [X_2]	NaCl (M) [X_3]	Turbidity removal (%)			Color removal (%)		
				0.5 mL	1.0 mL	1.5 mL	0.5 mL	1.0 mL	1.5 mL
1	12	6	1.0	71.1	62.6	72.5	9.6	16.4	16.4
2	12	8	1.0	64.8	57.9	61.2	9.0	15.1	18.5
3	12	7	0.5	54.7	54.4	61.6	12.0	21.1	25.0
4	12	7	1.5	63.6	59.4	55.4	7.8	13.0	14.9
5	24	6	0.5	75.4	77.5	77.5	10.4	47.0	23.0
6	24	8	0.5	79.9	70.2	72.0	4.0	15.3	20.7
7	24	6	1.5	59.7	63.8	66.3	14.0	14.2	17.0
8	24	8	1.5	62.1	49.6	61.9	8.1	24.0	17.2
9 (PC)	24	7	1.0	65.2	59.7	56.5	20.6	22.0	26.4
10 (PC)	24	7	1.0	71.9	62.7	59.0	9.2	13.1	15.3
11 (PC)	24	7	1.0	59.4	52.6	70.1	10.3	14.6	18.8
12 (PC)	24	7	1.0	60.7	68.0	69.2	7.6	14.0	16.3
13 (PC)	24	7	1.0	69.9	70.1	73.8	10.5	13.6	18.4
14	36	6	1.0	72.9	65.4	62.8	6.5	10.3	14.2
15	36	8	1.0	77.4	67.6	66.5	9.7	13.7	17.0
16	36	7	0.5	77.1	64.8	68.2	8.9	15.5	21.0
17	36	7	1.5	73.7	69.0	64.4	10.5	16.2	15.1

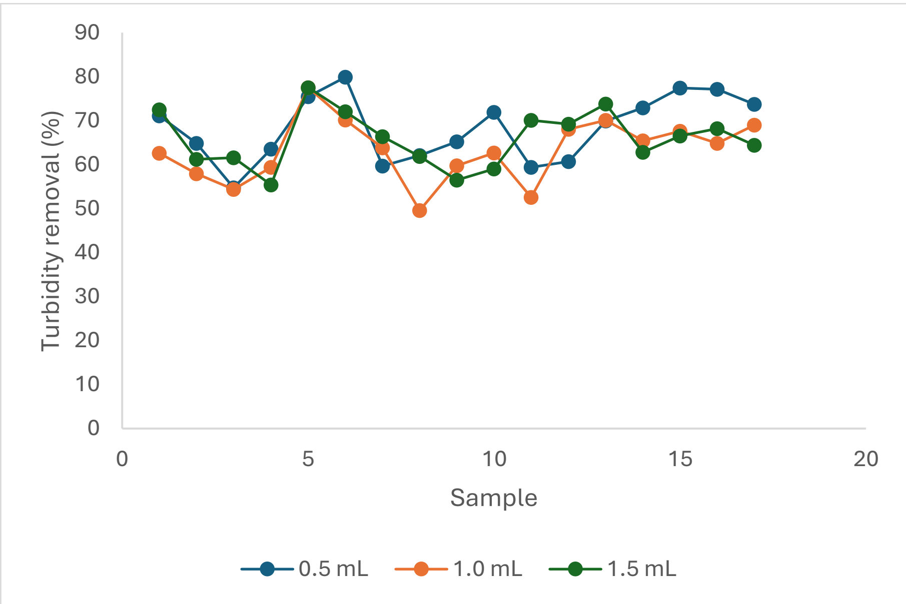

Figure 11. Turbidity removal using different walnut shell dosages.

The walnut shell biocoagulant demonstrated satisfactory turbidity removal under all evaluated operational conditions. At a dosage of 0.5 mL, the turbidity removal efficiency ranged from approximately 55 to 80%. The highest turbidity removal efficiency at this dosage was observed in experimental run 6 of the BBD, corresponding to an extraction time of 24 h, coagulation pH of 7, and a NaCl concentration of 0.5 M. This suggests that low NaCl concentrations combined with moderate-to-long extraction times favored the extraction of active coagulating compounds from walnut shells.

The experimental results indicated that acidic conditions generally favored higher coagulation performance, although near-neutral pH also produced efficiencies comparable to specific combinations of extraction time and NaCl concentration. This behavior may be associated with the ionization of phenolic and carboxylic functional groups present in the lignocellulosic biomass. Variations in pH alter the surface charge of the biopolymer, enhancing charge neutralization and polymer bridging mechanisms between suspended particles and natural coagulants.

For a dosage of 1.0 mL, the turbidity removal efficiencies varied between 50 and 78%. The highest efficiency was observed in run 5 under an extraction time of 24 h, pH 5, and NaCl concentration of 0.5 M. Compared with the 0.5 mL dosage, the 1.0 mL dosage demonstrated considerable variability in coagulation performance, suggesting sensitivity to the interaction effects among the operational parameters.

At a dosage of 1.5 mL, the turbidity removal efficiency ranged from 55 to 78%. The highest efficiency was obtained in run 5, which corresponded to an extraction time of 24 h, coagulation pH of 5, and NaCl concentration of 0.5 M. Other elevated efficiencies were also observed in run 13 (24 h, pH 6, 1.0 M NaCl), run 1 (12 h, pH 5, 1.0 M NaCl), and run 6 (24 h, pH 7, 0.5 M NaCl). These variations indicate that coagulation performance is strongly dependent on the interaction between extraction time, pH, and ionic strength, rather than being governed solely by the coagulant dosage.

The experimental data suggest that walnut shell extracts possess considerable coagulation potential due to the presence of tannins, lignin derivatives, cellulose, and hemicellulose compounds capable of promoting adsorption and charge neutralization mechanisms.

Some experimental conditions demonstrated reductions in efficiency at higher dosages; for example, run 4 presented lower efficiency at 1.5 mL than that at 0.5 mL. This behavior may indicate particle restabilization caused by excessive coagulant concentrations and charge-reversal phenomena. The central point experiments also demonstrated relatively consistent behavior, confirming the adequacy of the experimental design and the reproducibility of the central point runs.

4.2.2 ANOVA Analysis

The ANOVA results for the walnut shell biocoagulant showed that its performance depended on the dosage and response variable. Turbidity (Table 4) and color removal (Table 5) exhibited distinct statistical behaviors."

Table 4. Turbidity removal using walnut shells (ANOVA analysis).

Coagulant Dose (mL)	Model F-value	Model p-value	R^2 (%)	R^2adj (%)	Lack-of-fit p-value	Significant Factors
0.5	1.16	0.434	59.77	8.04	0.184	None
1.0	0.54	0.811	40.82	0.00	0.257	None
1.5	0.89	0.577	53.28	0.00	0.767	None

Table 5. Color removal using walnut shells (ANOVA analysis).

Coagulant Dose (mL)	Model F-value	Model p-value	R^2 (%)	R^2adj (%)	Lack-of-fit p-value	Significant Factors
0.5	0.27	0.964	25.85	0.00	0.685	None
1.0	4.49	0.030	85.24	66.27	0.179	$NaCl^2$ ($p = 0.036$); pH × NaCl ($p = 0.004$)
1.5	1.05	0.484	57.52	2.91	0.886	$NaCl^2$ ($p = 0.037$)

For turbidity removal, none of the developed quadratic models were statistically significant at the 95% confidence level, with model p-values of 0.434 (0.5 mL), 0.811 (1.0 mL), and 0.577 (1.5 mL). These results indicate that the evaluated independent variables of extraction time, pH, and NaCl concentration were insufficient to explain the variability in turbidity removal under the studied experimental conditions.

In addition, the adjusted coefficients of determination (R^2adj) were very low, ranging from 0 to 8%, confirming the limited explanatory and predictive capacities of the developed models. Although the models were not statistically significant, the lack-of-fit tests were not significant for any of the dosages, with $p = 0.184$, 0.257, and 0.767 for 0.5, 1.0, and 1.5 mL, respectively, indicating that no systematic deviation between the experimental and predicted values was observed.

Different statistical behaviors were observed for color removal depending on the coagulant dosage. The model corresponding to the 0.5 mL dosage was not statistically significant ($p = 0.964$) and showed a low explanatory power of $R^2 = 25.9\%$ and $R^2adj = 0.0\%$, indicating limited performance.

In contrast, the 1.0 mL dosage exhibited the most statistically robust behavior, with a significant model of $p = 0.030$, a high coefficient of determination of $R^2 = 85.2\%$, and a satisfactory adjusted coefficient of $R^2adj = 66.3\%$, indicating good model adequacy for this condition.

Under these conditions, the quadratic effect of NaCl concentration was statistically significant ($p = 0.036$), indicating a nonlinear influence of ionic strength on color removal efficiency. Moreover, the interaction between pH and NaCl concentration had a highly significant effect, representing the most influential term in this model. These results indicate that color removal is influenced by the combined effect of pH-dependent surface charge and ionic strength, which affect the adsorption and destabilization mechanisms of the dye molecules.

For the 1.5 mL dosage, the overall model was not statistically significant ($p = 0.484$), and the adjusted coefficient of determination was very low ($R^2 adj = 2.91\%$), indicating poor predictive reliability. However, NaCl concentration remained statistically significant as an individual factor ($p = 0.037$), suggesting that ionic strength may still influence dye removal under higher coagulant dosage conditions, although the overall model did not strongly support this.

Overall, the ANOVA results indicate that walnut shell biomass exhibits greater statistical robustness for color removal than for turbidity removal. The most consistent statistically relevant behavior was observed at the intermediate dosage of 1.0 mL, where the pH × NaCl interaction was identified as the most influential factor within the studied range.

4.2.3 Response Surface Methodology (RSM) and Contour Plot Analysis for Turbidity

The contour plots presented in Figures 12, 13, and 14 illustrate the effects of extraction pH, extraction time, and NaCl concentration on turbidity removal efficiency using walnut shell biocoagulants at dosages of 0.5, 1.0, and 1.5 mL, respectively. These plots provide a two-dimensional representation of the interaction effects among the evaluated operational variables, allowing the identification of optimal response regions and progressive changes in coagulation behavior as biocoagulant dosage increased.

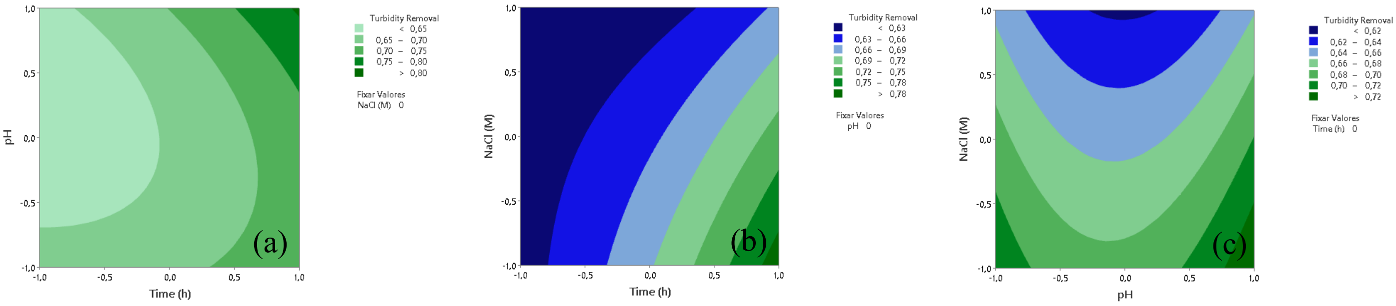

Figure 12. Contour plots for turbidity removal efficiency using walnut shell biocoagulant (0.5 mL dosage) as a function of: (a) pH vs. time; (b) NaCl concentration vs. time; (c) NaCl concentration vs. pH.

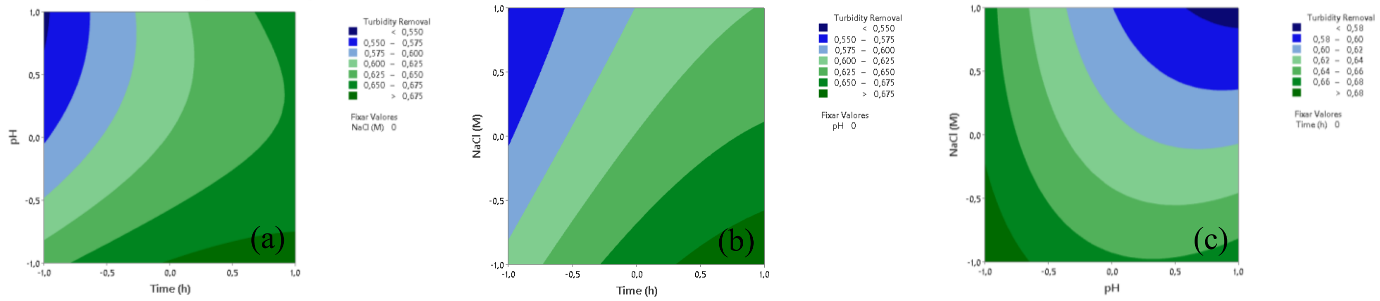

Figure 13. Contour plots for turbidity removal efficiency using walnut shell biocoagulant (1.0 mL dosage) as a function of: (a) pH vs. time; (b) NaCl concentration vs. time; (c) NaCl concentration vs. pH.

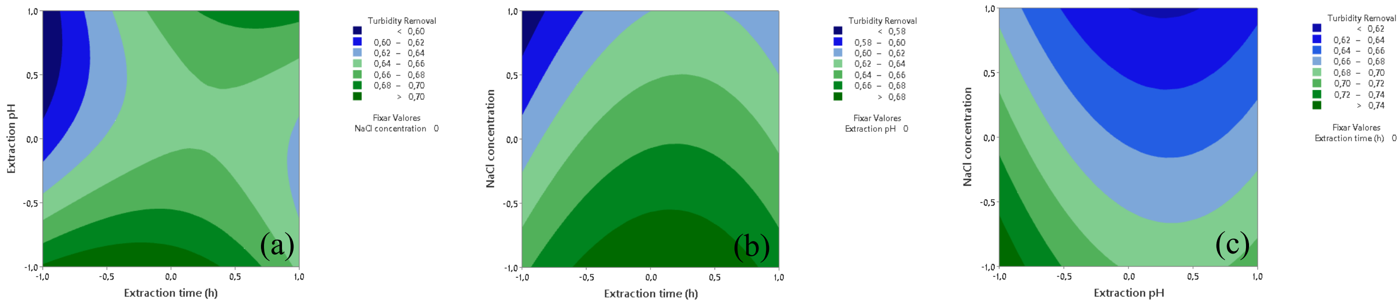

Figure 14. Contour plots for turbidity removal efficiency using walnut shell biocoagulant (1.5 mL dosage) as a function of: (a) pH vs. time; (b) NaCl concentration vs. time; (c) NaCl concentration vs. pH.

The turbidity removal efficiency was strongly influenced by the interaction between extraction pH, extraction time, and NaCl concentration. However, the response behavior progressively changed according to the applied coagulant dosage, indicating that the relative influence of the extraction variables on coagulation performance was modified.

At the lowest dosage (Figure 12), broader optimal response regions were observed, indicating the greater sensitivity of turbidity removal efficiency to variations in extraction conditions. The highest efficiencies (>0.80) were generally associated with alkaline extraction conditions (pH 8), prolonged extraction times (36 h), and low NaCl concentrations (0.5 M). In particular, the interaction between extraction time and NaCl concentration demonstrated that extended extraction periods combined with reduced ionic strength favored clarification efficiency, suggesting improved extraction and availability of active coagulating compounds.

In contrast, the contour plots obtained at 1.0 mL dosage (Figure 13) exhibited more localized optimal regions and a more pronounced influence of acidic extraction conditions, particularly near pH 6. The highest turbidity removal efficiencies (>0.68) were observed under low NaCl concentrations combined with extraction times of approximately 36 h. Although extraction time still positively influenced coagulation performance, the dependence on prolonged extraction periods appeared to decrease compared with that of 0.5 mL dosage.

At the highest dosage (Figure 14), the contour plots exhibited a more homogeneous and stable response profile, with the highest turbidity removal efficiencies (>0.74) predominantly observed under acidic extraction conditions (pH 6), low NaCl concentrations (0.5 M), and intermediate extraction times. These results indicate that increasing the biocoagulant dosage progressively reduced the sensitivity of the system to extraction time, while enhancing the influence of extraction pH on coagulation performance.

Overall, the contour plots indicate that increasing the walnut shell biocoagulant dosage progressively reduced the sensitivity of turbidity removal efficiency to extraction time while enhancing the influence of extraction pH on coagulation performance. The interaction effects observed among pH, extraction time, and NaCl concentration reinforce the importance of multivariate optimization in natural coagulant extraction processes. Similar behaviors have been reported for lignocellulosic and plant-based coagulants, where coagulation performance is strongly associated with colloidal destabilization, charge neutralization, and floc formation mechanisms (Yin, 2010; Choy et al., 2014; Benalia et al., 2024; Mohammad Ali et al., 2024). According to Zourif et al. (2024), turbidity removal using walnut-derived biocoagulants is predominantly related to particle destabilization and coagulation–flocculation mechanisms, which leads to the precipitation and removal of suspended matter. In addition, natural polymers, such as proteins and polysaccharides, may contribute to interparticle bridging and aggregation phenomena, favoring floc formation and clarification efficiency (Choy et al., 2014). These mechanisms may explain the progressive stabilization of the response behavior and reduction in dependence on prolonged extraction times observed at higher biocoagulant dosages.

Due to the statistical non-significance of the quadratic regression model in the ANOVA analysis, the three-dimensional RSM surfaces were replaced by experimental trend plots based directly on the observed experimental data, as shown in Figures 15, 16 and 17. Because the Box–Behnken experimental design does not provide fully fixed central-point conditions for all operational variables simultaneously, the plots were constructed using the average turbidity removal efficiencies obtained at each evaluated operational level. This approach allows for a clearer visualization of the overall experimental tendencies associated with extraction time, extraction pH, and NaCl concentration, while preserving the multivariate nature of the experimental design. In addition, these plots provide a more reliable representation of the actual experimental behavior of the system, highlighting trends and operational effects that the quadratic regression model cannot fully capture.

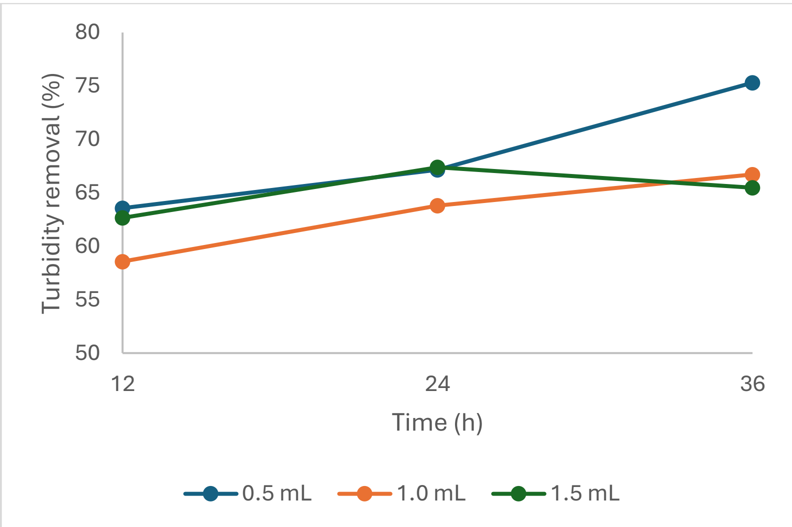

Figure 15. Effect of extraction time on turbidity removal.

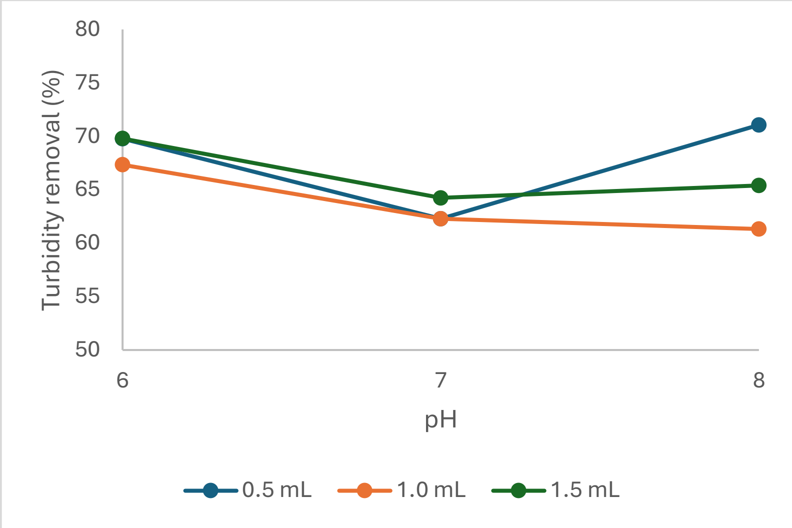

Figure 16. Effect of extraction pH on turbidity removal.

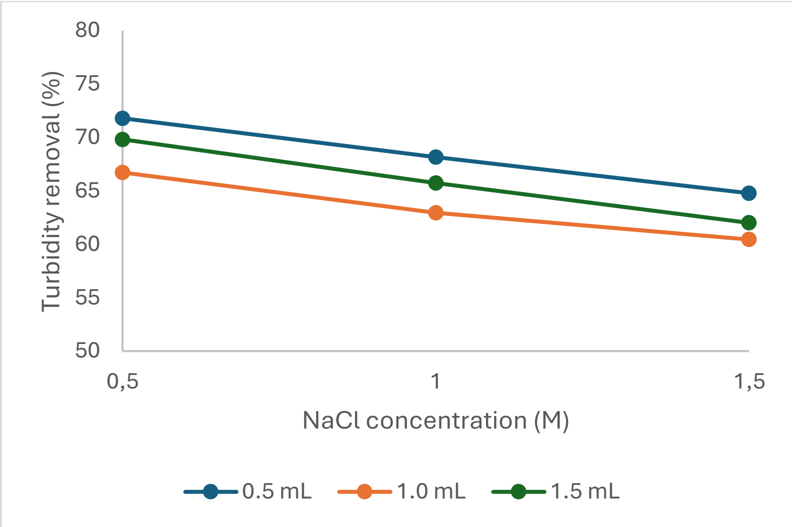

Figure 17. Effect of NaCl concentration on turbidity removal.

Overall, the experimental trend plots strongly corroborate the tendencies previously identified in the contour plots, reinforcing the consistency of the observed operational behavior, despite the statistical limitations of the quadratic regression model. Both graphical approaches consistently demonstrated that prolonged extraction times and low NaCl concentrations favored turbidity removal efficiency, particularly at the 0.5 mL dosage level. Likewise, the plots also indicate that increasing the walnut shell biocoagulant dosage progressively reduced the sensitivity of the system to extraction time while enhancing the relative influence of extraction pH on coagulation performance.

Specifically, the contour plots in Figure 12 suggest that the highest turbidity removal efficiencies at the 0.5 mL dosage were associated with prolonged extraction times and low NaCl concentrations, and this tendency is directly confirmed by the experimental trend plots presented in Figures 15 and 17. Similarly, the alkaline conditions observed in these contour plots are also reflected in Figure 16, where a pH of 8 exhibited the highest average turbidity removal efficiency at a 0.5 mL dosage.

At higher dosages, both graphical approaches consistently indicated progressive stabilization of the coagulation system. In the contour plots corresponding to Figures 13 and 14, the optimal operational regions became more localized and less dependent on prolonged extraction periods. This behavior is evident in Figure 15, where the variation in turbidity removal efficiency with extraction time became less evident at 1.0 and 1.5 mL. In addition, the contour plots suggested that acidic extraction conditions became progressively more favorable at higher dosages, which is also supported by Figure 16, where the differences between pH conditions became smaller, and the response behavior was more stable.

Furthermore, the negative influence of increasing NaCl concentration observed in the contour plots is consistently reproduced in Figure 17, where all evaluated dosages exhibited a reduced turbidity removal efficiency with increasing salt concentration. This agreement between the contour plots and experimental trend plots reinforces the interpretation that reduced ionic strength favors the preservation or activity of the functional compounds responsible for coagulation and floc formation.

Together, these complementary graphical analyses strengthen the interpretation of the experimental behavior of the walnut shell biocoagulant system, demonstrating strong consistency between the multivariable contour analysis and the direct experimental trends obtained from the observed data.

4.2.4 Response Surface Methodology (RSM) and Contour Plot Analysis for Color

The contour plots presented in Figures 18, 19, and 20 illustrate the effects of extraction pH, extraction time, and NaCl concentration on color removal efficiency using walnut shell biocoagulant at 0.5, 1.0, and 1.5 mL dosages. These plots provide a two-dimensional representation of the interaction effects among the evaluated operational variables, allowing the identification of optimal response regions and progressive changes in color removal behavior as the biocoagulant dosage increased.

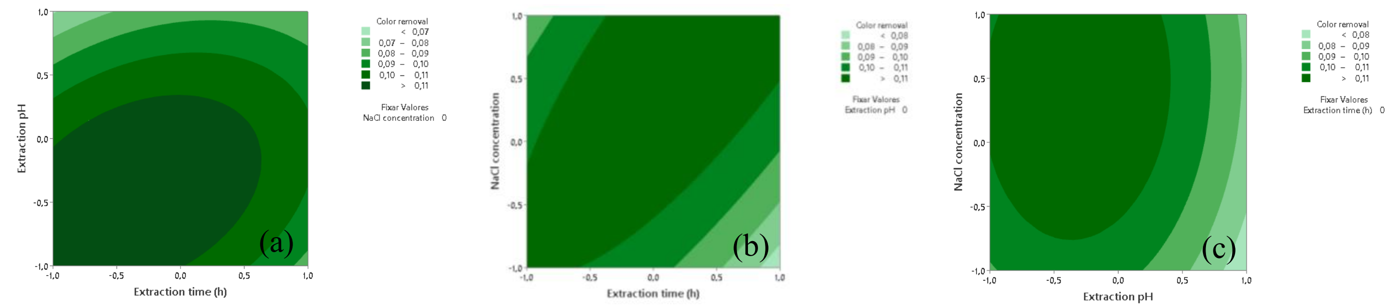

Figure 18. Contour plots for color removal efficiency using walnut shell biocoagulant (0.5 mL dosage) as a function of: (a) pH vs. time; (b) NaCl concentration vs. time; (c) NaCl concentration vs. pH.

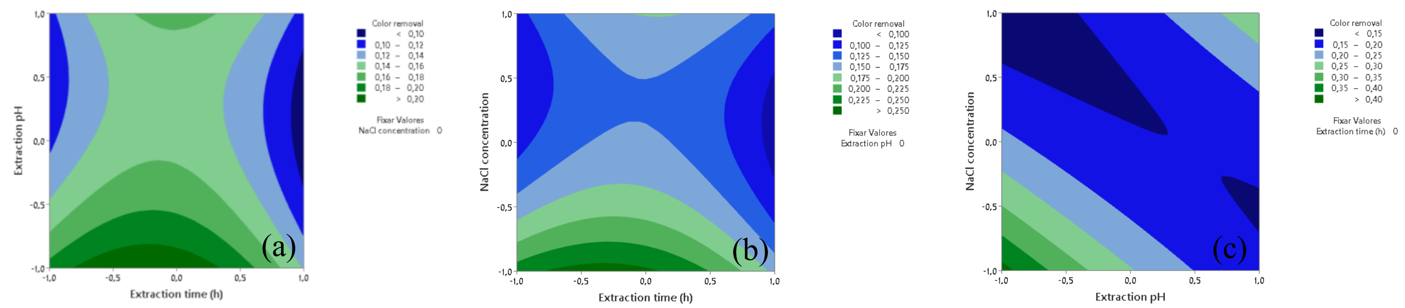

Figure 19. Contour plots for color removal efficiency using walnut shell biocoagulant (1.0 mL dosage) as a function of: (a) pH vs. time; (b) NaCl concentration vs. time; (c) NaCl concentration vs. pH.

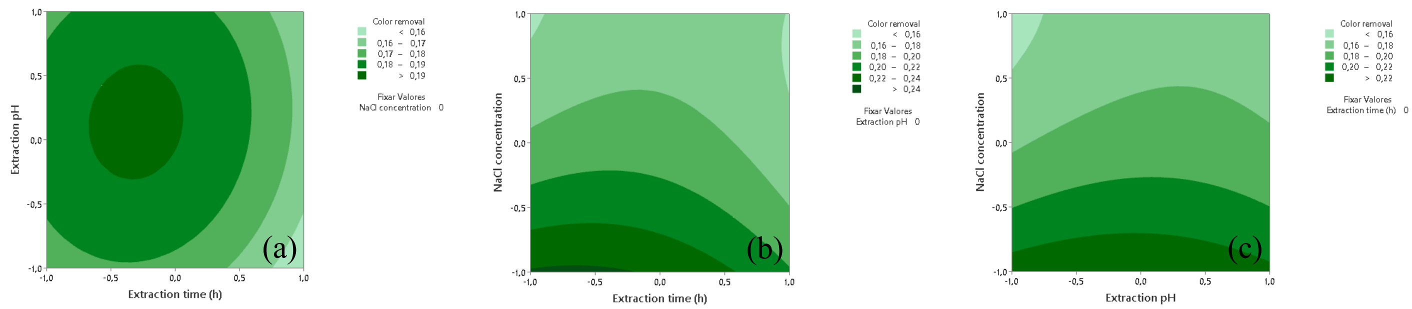

Figure 20. Contour plots for color removal efficiency using walnut shell biocoagulant (1.5 mL dosage) as a function of: (a) pH vs. time; (b) NaCl concentration vs. time; (c) NaCl concentration vs. pH.

The color removal efficiency was strongly influenced by the interactions between extraction pH, extraction time, and NaCl concentration. However, the response behavior progressively changed according to the applied coagulant dosage, indicating modifications in the relative contribution of the extraction variables to the coagulation performance.

At the lowest dosage (Figure 18), broader and more symmetric optimal response regions were observed, indicating a greater sensitivity of color removal efficiency to variations in extraction conditions. The contour plots exhibited elliptical and paraboloidlike response regions, particularly for the pH–time and NaCl–pH interactions, suggesting complex nonlinear behaviors among the evaluated variables. The highest color removal efficiencies (>0.11) were generally associated with moderately acidic to near-neutral extraction conditions (pH 6–7.25), intermediate extraction times (12–27 h), and intermediate to high NaCl concentrations (0.75–1.5 M). In addition, equivalent optimal responses were observed for distinct combinations of extraction time and ionic strength, reinforcing the presence of interaction-dependent operational regions and strong nonlinear system behavior.

At the intermediate dosage (Figure 19), the contour plots became more concentrated and exhibited steeper gradient responses. Acidic extraction conditions near pH 6 became considerably more influential, particularly when combined with low NaCl concentrations (0.5 M) and intermediate extraction times ranging from approximately 18 to 24 h. The highest color removal efficiencies (>0.40) were obtained under the combined effect of acidic extraction conditions and reduced ionic strength, suggesting a strong synergistic interaction between pH and NaCl concentration. Compared with the 0.5 mL dosage, the optimal regions became narrower and more localized, indicating the progressive stabilization of the coagulation process. The diagonal response pattern observed in the NaCl–pH interaction plot also suggests a stronger synergistic interaction between the ionic strength and extraction pH at this dosage.

At the highest dosage (Figure 20), the contour plots exhibited more homogeneous and stable response regions with smoother transitions between the operational conditions. In contrast to the lower dosages, the system was predominantly governed by NaCl concentration, as the highest color removal efficiencies (>0.24) were consistently achieved at the lowest NaCl concentration evaluated (0.5 M), regardless of moderate variations in extraction pH and extraction time. The optimal regions also became broader and less dependent on strongly acidic conditions, with near-neutral pH values and intermediate extraction times remaining favorable for color removal. These results suggest that increasing the coagulant dosage progressively reduced the sensitivity of the system to extraction parameter variations, while reinforcing the dominant role of ionic strength in the adsorption-related removal mechanisms.

Overall, the contour plots indicate that increasing the walnut shell biocoagulant dosage progressively enhanced the stability of the color removal process while reducing the dependence on extensive extraction conditions. Furthermore, the progressive dominance of low NaCl concentrations at higher dosages suggests that a reduced ionic strength favors the preservation or extraction of functional groups associated with color removal. According to Yin (2010), salt-assisted extraction may alter the solubility and dissociation of coagulating compounds through salting-in effects, directly influencing the extraction efficiency of active substances under different ionic strengths. In walnut-derived biocoagulants, compounds such as tannins, polyphenols, proteins, and polysaccharides may provide adsorption sites capable of interacting with dissolved colored molecules through electrostatic interactions and surface adsorption mechanisms (Zourif et al., 2024). Choy et al. (2014) reported that plant-based coagulants rich in natural polymers exhibit adsorption-related removal mechanisms that are strongly influenced by extraction conditions and solution chemistry. These mechanisms may explain the progressive stabilization of the response surfaces and the strong influence of NaCl concentration observed at higher biocoagulant dosage.

To complement the contour plot analysis, additional experimental trend plots were constructed from the observed color removal data, as shown in Figures 21, 22, and 23. The plots were generated using the average removal efficiencies obtained at each operational level, allowing the identification of general response tendencies while preserving the multivariate characteristics of the Box–Behnken experimental design.

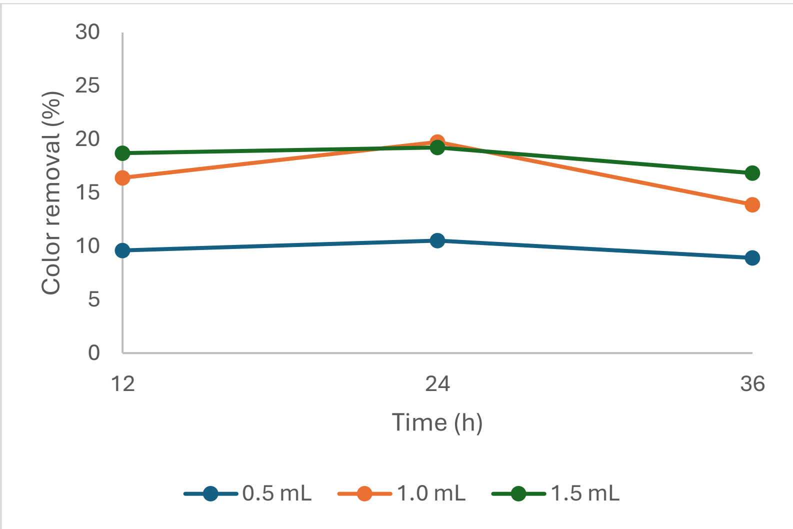

Figure 21. Effect of extraction time on color removal.

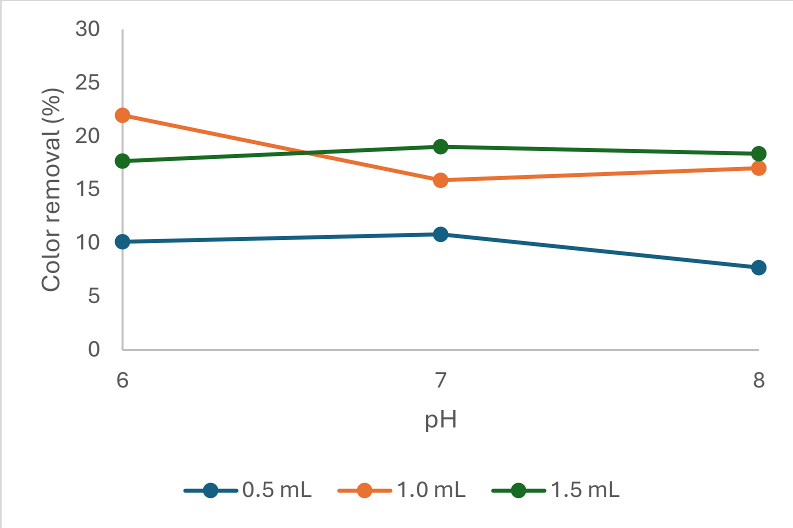

Figure 22. Effect of extraction pH on color removal.

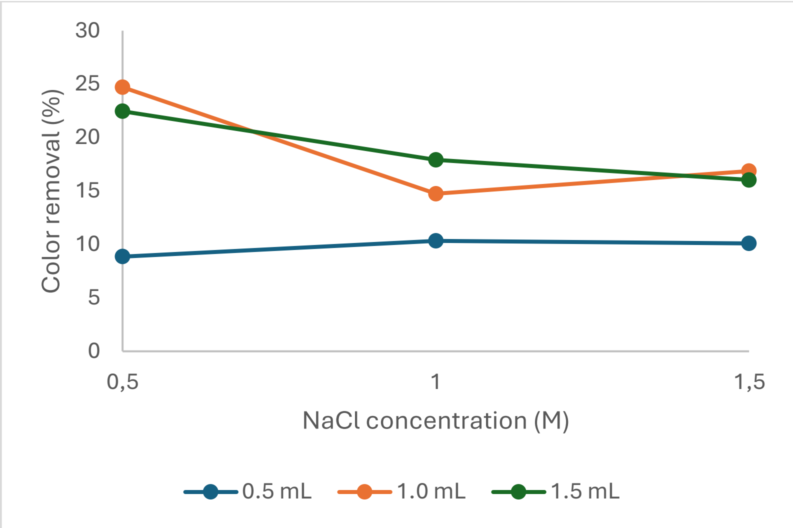

Figure 23. Effect of NaCl concentration on color removal.

The contour plots in Figure 18 suggest that intermediate extraction times and moderate-to-high NaCl concentrations favored color removal at the lowest dosage. This tendency is directly reflected in Figure 21, where the 0.5 mL dosage exhibited only slight variation with extraction time, while the 1.0 and 1.5 mL dosages achieved their highest average color removal efficiencies at an extraction time of approximately 24 h. Similarly, the broader and more symmetric optimal regions observed in the contour plots at the 0.5 mL dosage are also reflected in the smoother experimental trends shown in Figs. 21 and 22.

At the intermediate dosage, the contour plots in Figure 19 demonstrate that acidic extraction conditions combined with low NaCl concentrations produced the highest color removal efficiencies, and this tendency is confirmed by Figures 22 and 23.

At the highest dosage, both graphical approaches consistently indicated progressive stabilization of the coagulation system. The contour plots in Figure 20 suggested that low NaCl concentrations became the main favorable condition for color removal regardless of moderate variations in pH and extraction time. This behavior is directly corroborated by Figure 23. In addition, Figures 21 and 22 demonstrated smoother response variations at the highest dosage, reinforcing the more homogeneous and stable operational behavior identified in the contour plots.

4.3 Eucalyptus Bark Biocoagulant

4.3.1 Turbidity Removal Performance

The eucalyptus bark biocoagulant demonstrated excellent turbidity removal under the evaluated operational conditions. Table 6 and Figure 24 present the results for the eucalyptus bark. The experimental results indicated that the coagulation efficiency was influenced by the extraction time, coagulation pH, KCl concentration, and coagulant dosage.

Table 6. Turbidity and color removal by eucalyptus bark.

Sample	Time (h) [X_1]	pH [X_2]	KCl (M) [X_3]	Turbidity removal (%)			Color removal (%)		
				0.5 mL	1.0 mL	1.5 mL	0.5 mL	1.0 mL	1.5 mL
1	12	5	1.0	61.5	56.8	60.1	14.3	33.7	40.3
2	12	7	1.0	58.0	53.4	66.6	22.7	35.3	47.5
3	12	6	0.5	67.3	50.7	55.7	12.8	26.8	40.2
4	12	6	1.5	61.9	53.6	51.4	14.2	23.2	34.7
5	24	5	0.5	63.5	60.9	60.9	16.8	25.1	35.6
6	24	7	0.5	63.1	64.7	60.0	19.1	44.0	36.4
7	24	5	1.5	62.7	67.6	74.1	13.6	25.4	34.2
8	24	7	1.5	69.7	69.8	71.9	17.2	21.6	32.1
9 (PC)	24	6	1.0	57.8	52.1	50.5	9.6	16.6	23.7
10 (PC)	24	6	1.0	62.8	63.0	64.8	16.7	19.8	25.1
11 (PC)	24	6	1.0	58.0	59.1	65.9	12.7	20.7	29.5
12 (PC)	24	6	1.0	63.8	55.5	63.0	10.3	15.1	20.0
13 (PC)	24	6	1.0	61.5	61.2	59.0	7.4	12.1	17.9
14	36	5	1.0	90.4	79.5	84.2	12.5	21.0	26.0
15	36	7	1.0	64.5	82.8	77.8	11.8	19.3	24.4
16	36	6	0.5	57.3	54.6	66.2	8.3	15.7	20.4
17	36	6	1.5	67.6	64.1	64.0	9.8	15.5	25.3

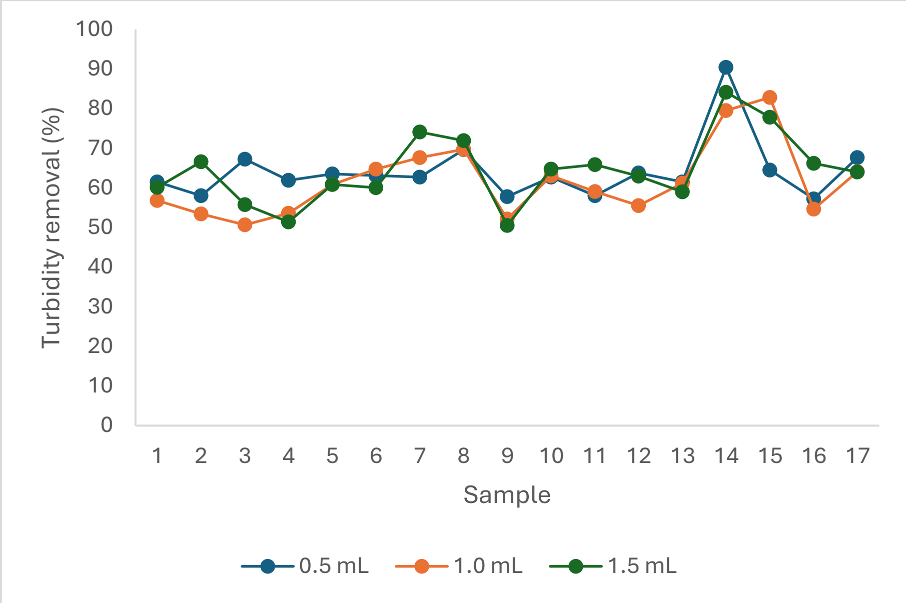

Figure 24. Turbidity removal using different eucalyptus bark dosage.

For a dosage of 0.5 mL, turbidity removal efficiencies ranged from 57% in run 16 with an extraction time of 36 h, pH 6, and 0.5 M KCl, to 90% in run 14 with an extraction time of 36 h, pH 5, and 1.0 M KCl. The highest performance observed in Run 14 suggests that prolonged extraction time combined with acidic conditions and intermediate ionic strength enhanced the release and activity of coagulating compounds from eucalyptus bark biomass.

The results further indicated that both acidic and near-neutral pH conditions produced high efficiencies depending on the interaction with other operational variables. This behavior may be associated with the protonation state of the functional groups in lignocellulosic compounds and their interactions with suspended particles, influencing destabilization mechanisms.

For a dosage of 1.0 mL, turbidity removal efficiencies varied between 50% in run 3 with an extraction time of 12 h, pH 6, 0.5 M KCl and 83% in run 15 with an extraction time of 36 h, pH 7 and 1.0 M KCl. Compared with the 0.5 mL dosage, the 1.0 mL dosage showed a wide range of performance with several moderate-to-high efficiency values distributed across different experimental conditions, indicating effective floc formation under diverse operational conditions.

At a dosage of 1.5 mL, turbidity removal efficiencies ranged from 51% in run 9, the central point, to 84% in run 14 at an extraction time of 36 h, pH 5, and 1.0 M KCl.

High efficiencies were also observed in run 15 (78 %) and run 7 (74 %), indicating that higher dosages can enhance coagulation performance under specific combinations of operational parameters.

The experimental data suggest that eucalyptus bark extracts contain polyphenolic compounds, lignin derivatives, tannins, cellulose, and hemicellulose structures that promote adsorption, bridging, and charge neutralization mechanisms during particle destabilization. The KCl concentration had a nonlinear influence on turbidity removal, suggesting that ionic strength affects electrical double-layer compression and particle destabilization in a complex manner, depending on the interactions with pH and extraction conditions.

Additionally, longer extraction times tended to produce higher efficiencies for specific combinations of operational parameters, although the effect was not strictly monotonic across all experiments. This suggests that extraction kinetics play an important role in the availability of active compounds; however, their effectiveness depends on interactions with other operational variables.

The central point experiments showed moderate variability but acceptable reproducibility, confirming the consistency of our experimental design. Overall, the results indicate that eucalyptus bark biomass is a promising natural biocoagulant for turbidity removal under favorable operational conditions.

4.3.2 Eucalyptus Bark ANOVA Results

The statistical analysis performed for the eucalyptus bark biocoagulant revealed that the model performance varied depending on both the response variable and the coagulant dosage, with distinct behaviors observed for turbidity (Table 7) and color removal (Table 8).

Table 7. Turbidity removal using eucalyptus bark (ANOVA).

Coagulant Dose (mL)	Model F-value	Model p-value	R^2 (%)	R^2adj (%)	Lack-of-fit p-value	Significant Factors
0.5	1.08	0.469	58.20	4.46	0.011	None
1.0	3.28	0.066	80.85	56.23	0.150	Extraction time (p = 0.006); pH^2 (p = 0.012)
1.5	2.47	0.123	76.07	45.31	0.405	Extraction time (p = 0.016); pH^2 (p = 0.021)

Table 8. Color removal using eucalyptus bark (ANOVA).

Coagulant Dose (mL)	Model F-value	Model p-value	R^2 (%)	R^2adj (%)	Lack-of-fit p-value	Significant Factors
0.5	2.57	0.114	76.73	46.82	0.841	Extraction time (p = 0.036); pH^2 (p = 0.014)
1.0	5.69	0.016	87.98	72.51	0.223	Extraction time (p = 0.006); pH^2 (p = 0.003); pH × NaCl (p = 0.034)
1.5	8.13	0.006	91.27	80.05	0.802	Extraction time (p < 0.001); pH^2 (p = 0.006)

For turbidity removal, the 0.5 mL dosage did not produce a statistically significant model (p = 0.469). In addition, the lack-of-fit test was significant (p = 0.011), indicating possible model inadequacy and limitations in the model structure. At the 1.0 mL dosage, the model was not statistically significant (p = 0.066), although it exhibited high explanatory capacity (R^2 = 80.85% and R^2 adj = 56.23 %). Under these conditions, extraction time (p = 0.006) and the quadratic effect of pH (p = 0.012) were statistically significant, indicating relevant contributions within the experimental domain. A similar pattern was observed for the 1.5 mL dosage, where the model remained not statistically significant (p = 0.123), although extraction time (p = 0.016) and the quadratic effect of pH (p = 0.021) continued to be statistically significant.

Overall, the turbidity removal results suggest a dependence on extraction time and pH-dependent nonlinear effects; however, the model significance varies across dosages, indicating lower overall statistical significance and variability in model performance.

The statistical behavior for color removal was considerably stronger than that for turbidity removal, particularly at 1.0 and 1.5 mL dosages. For the 0.5 mL dosage, the model was not statistically significant ($p = 0.114$), although it showed moderate explanatory capacity ($R^2 = 76.73\%$ and R^2 adj = 46.82 %). Under these conditions, extraction time ($p = 0.036$) and the quadratic effect of pH ($p = 0.014$) were statistically significant, indicating an influence on dye removal even at low dosage levels.

At the 1.0 mL dosage, the model exhibited statistically significant behavior with $p = 0.016$, with a high explanatory capacity of $R^2 = 87.98\%$ and $R^2adj = 72.51\%$. Extraction time $p = 0.006$, pH^2 $p = 0.003$, and the interaction between pH and NaCl concentration $p = 0.034$, were statistically significant, indicating the combined effects of the operational variables.

At the 1.5 mL dosage, the model presented the highest coefficient of determination $R^2 = 91.27\%$ and $R^2adj = 80.05\%$ and was statistically significant ($p = 0.006$). Under these conditions, extraction time ($p < 0.001$) and the quadratic effect of pH ($p = 0.006$) were both highly significant. All color removal models exhibited non-significant lack-of-fit values ($p > 0.05$), indicating a good agreement between the experimental data and model predictions.

Overall, eucalyptus bark biomass demonstrated a stronger statistical performance for color removal than for turbidity removal, particularly at 1.0 and 1.5 mL dosages. The results suggest that color removal is more sensitive to process optimization variables, especially extraction time and pH, whereas turbidity removal shows greater variability and lower statistical robustness.

4.3.3 Response Surface Methodology (RSM) and Contour Plot Analysis for Turbidity

The contour plots presented in Figures 25, 26, and 27 illustrate the effects of extraction pH, extraction time, and KCl concentration on turbidity removal efficiency using eucalyptus bark biocoagulant at 0.5, 1.0, and 1.5 mL dosages, respectively. These plots provide a two-dimensional representation of the interaction effects among the evaluated operational variables, allowing the identification of optimal response regions and progressive changes in coagulation behavior as biocoagulant dosage increased.

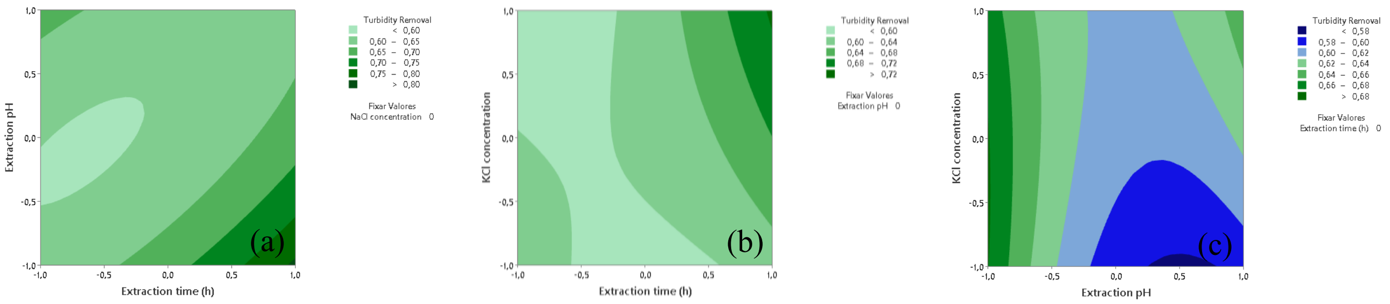

(a) (b) (c)

Figure 25. Contour plots for turbidity removal efficiency using eucalyptus bark biocoagulant (0.5 mL dosage) as a function of: (a) pH vs. time; (b) KCl concentration vs. time; (c) KCl concentration vs. pH.

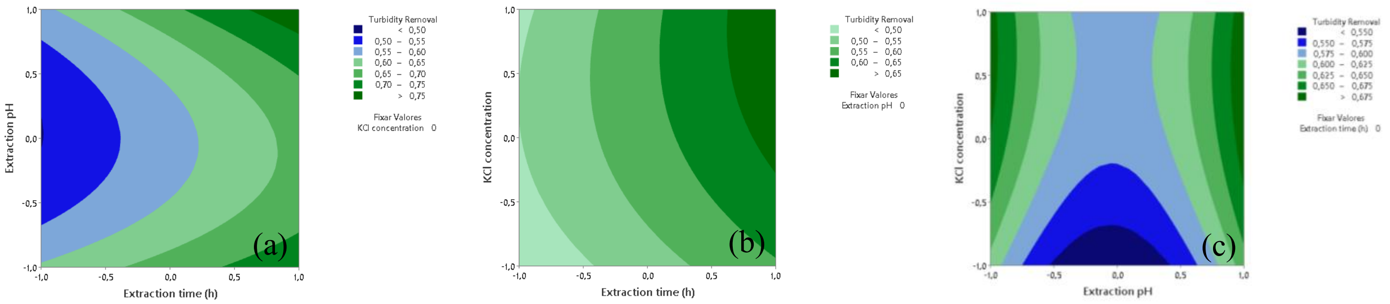

Figure 26. Contour plots for turbidity removal efficiency using eucalyptus bark biocoagulant (1.0 mL dosage) as a function of: (a) pH vs. time; (b) KCl concentration vs. time; (c) KCl concentration vs. pH.

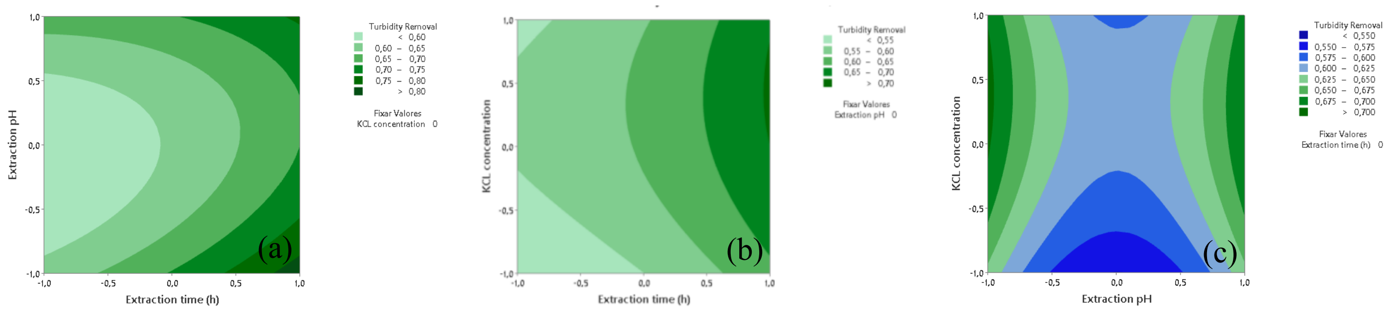

Figure 27. Contour plots for turbidity removal efficiency using eucalyptus bark biocoagulant (1.5 mL dosage) as a function of: (a) pH vs. time; (b) KCl concentration vs. time; (c) KCl concentration vs. pH.

Overall, the turbidity removal efficiency using eucalyptus bark biocoagulants was strongly influenced by the interactions among extraction pH, extraction time, and KCl concentration. However, the response behavior progressively changed according to the applied coagulant dosage, indicating that the relative influence of the extraction variables on coagulation performance was modified.

At the lowest dosage (Figure 25), broader and more heterogeneous optimal response regions were observed, indicating a greater sensitivity of the turbidity removal efficiency to variations in the extraction conditions. The highest turbidity removal efficiencies (>0.80) were generally associated with strongly acidic extraction conditions (pH 5), prolonged extraction times (36 h), and high KCl concentrations. In particular, the interaction between KCl concentration and extraction time demonstrated that increased ionic strength combined with an extended extraction duration positively influenced clarification efficiency, suggesting enhanced extraction and activation of bioactive coagulating compounds under these conditions. Effective coagulation performance (>0.68) was also observed at moderate KCl concentrations (0.5–1.0 M).

At the intermediate dosage (Figure 26), the contour plots became more concentrated and exhibited stronger nonlinear interaction effects between the evaluated variables. High turbidity removal efficiencies (>0.75) were achieved under both acidic and near-neutral extraction conditions, particularly when associated with prolonged extraction times (36 h) and intermediate-to-high KCl concentrations (1.0–1.5 M). One optimal region was associated with high KCl concentrations combined with acidic extraction conditions (pH 5), whereas a second region emerged under similar ionic strength conditions but near-neutral pH values (pH 7).

At the highest dosage (Figure 27), the response regions became more homogeneous and stable, whereas the optimal operational conditions remained predominantly associated with strongly acidic extraction pH (pH 5), prolonged extraction times (36 h), and intermediate-to-high KCl concentrations (>1.0 M). The highest turbidity removal efficiencies (>0.80) were consistently obtained under these conditions, reinforcing the synergistic interaction between the acidic extraction conditions and elevated ionic strength during the extraction process. Compared with the lower dosages, the system exhibited reduced sensitivity to moderate variations in the operational conditions, indicating progressive stabilization of coagulation behavior at higher eucalyptus bark biocoagulant dosages.

Overall, the contour plots indicate that turbidity removal using eucalyptus bark biocoagulants is strongly favored by acidic extraction conditions, prolonged extraction times, and moderate-to-high KCl concentrations. According to Yin (2010), salt-assisted extraction may improve the solubility and dissociation of coagulating compounds through salting-in effects, thereby enhancing the extraction efficiency of active substances under conditions of elevated ionic strength. Eucalyptus-derived biocoagulants are rich in tannins, flavonoids, proteins, polyphenols, and lignocellulosic compounds containing hydroxyl and carboxyl functional groups that promote colloidal destabilization, charge neutralization, and floc formation during coagulation–flocculation processes (Uwanta et al., 2022; Khelladi et al., 2026). Uwanta et al. (2022) reported that *Eucalyptus citriodora* exudates exhibited effective coagulation activity associated with their elevated phytochemical content, particularly tannins, proteins, resins, and flavonoids, which may contribute to particle aggregation and suspended matter destabilization during water purification. Similar interaction-dependent behaviors have been reported for plant-based and lignocellulosic coagulants, particularly regarding the influence of extraction conditions and ionic strength on coagulation efficiency (Yin, 2010; Choy et al., 2014; Benalia et al., 2024; Mohammad Ali et al., 2024). These mechanisms may explain the progressive stabilization of the response surfaces and the strong interaction effects observed among extraction pH, extraction time, and KCl concentration.

To further support the contour plot interpretation, complementary experimental trend plots based on the observed turbidity removal efficiencies were constructed (Figures 28, 29, and 30). These plots directly illustrate the influence of extraction time, extraction pH, and KCl concentration on turbidity removal performance at different eucalyptus bark biocoagulant dosages. The plots were generated using the average removal efficiencies obtained at each evaluated operational level, allowing a clearer visualization of the dominant experimental tendencies while preserving the multivariable characteristics of the Box–Behnken design.

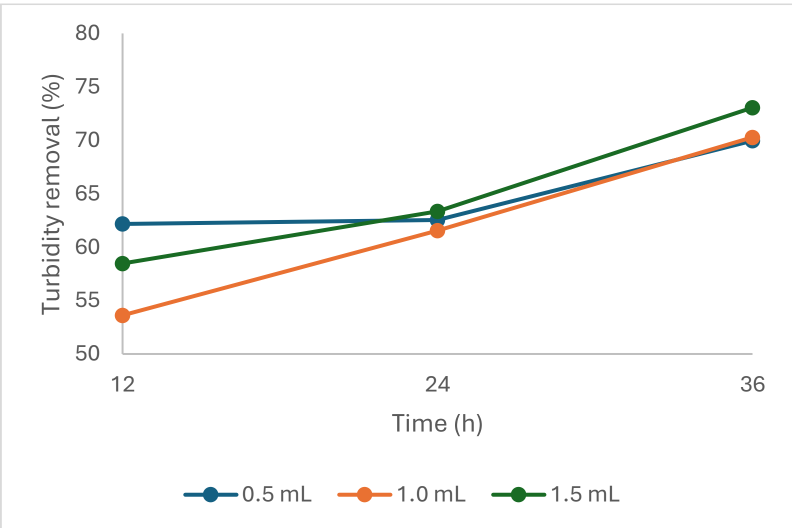

Figure 28. Effect of extraction time on turbidity removal.

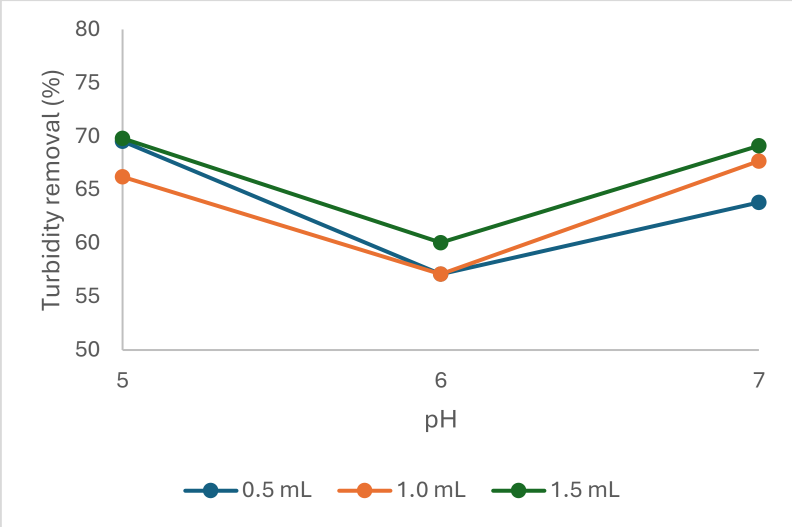

Figure 29. Effect of extraction pH on turbidity removal.

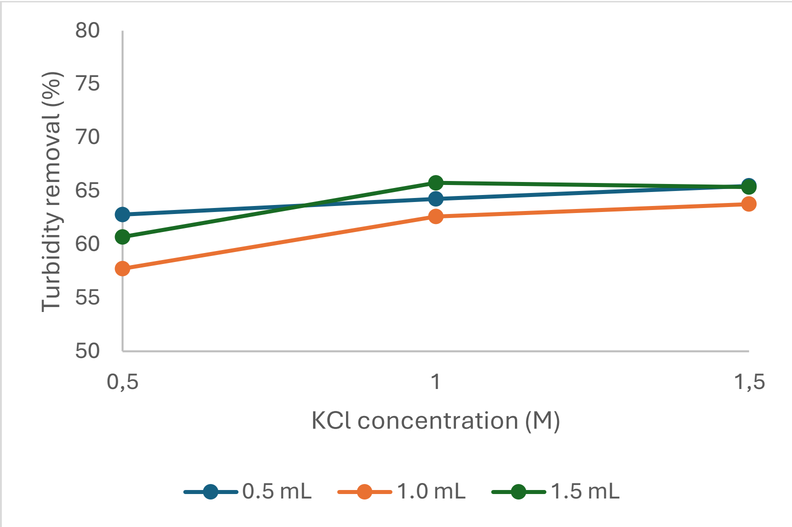

Figure 30. Effect of KCl concentration on turbidity removal.

Overall, the experimental trend plots strongly corroborated the tendencies previously identified in the contour plots, reinforcing the consistency of the operational behavior observed across the evaluated eucalyptus bark biocoagulant doses. Both graphical approaches consistently demonstrated that prolonged extraction times favored turbidity removal efficiency, particularly at 1.0 and 1.5 mL dosages. Likewise, both the contour and experimental trend plots indicated that acidic extraction conditions generally promoted higher turbidity removal efficiencies, whereas higher KCl concentrations positively influenced coagulation performance.

At the intermediate dosage, the contour plots in Figure 26 demonstrated more pronounced nonlinear interaction effects and the emergence of two optimal regions associated with both acidic and near-neutral conditions under elevated KCl concentrations. This behavior is also shown in Figure 29.

At the highest dosage, both graphical approaches consistently indicated progressive stabilization of the coagulation system. The contour plots in Figure 27 suggest that strongly acidic or near-neutral conditions, prolonged extraction times, and intermediate-to-high KCl concentrations remained the main favorable operational conditions, which is confirmed in Figures 28–30.

4.3.4 Response Surface Methodology (RSM) and Contour Plot Analysis for Color

The contour plots presented in Figures 31, 32, and 33 illustrate the effects of extraction pH, extraction time, and KCl concentration on color removal efficiency using eucalyptus bark biocoagulant at dosages of 0.5, 1.0, and 1.5 mL. These plots provide a two-dimensional representation of the interaction effects among the evaluated operational variables, allowing the identification of optimal response regions and progressive changes in color removal behavior as the biocoagulant dosage increased.

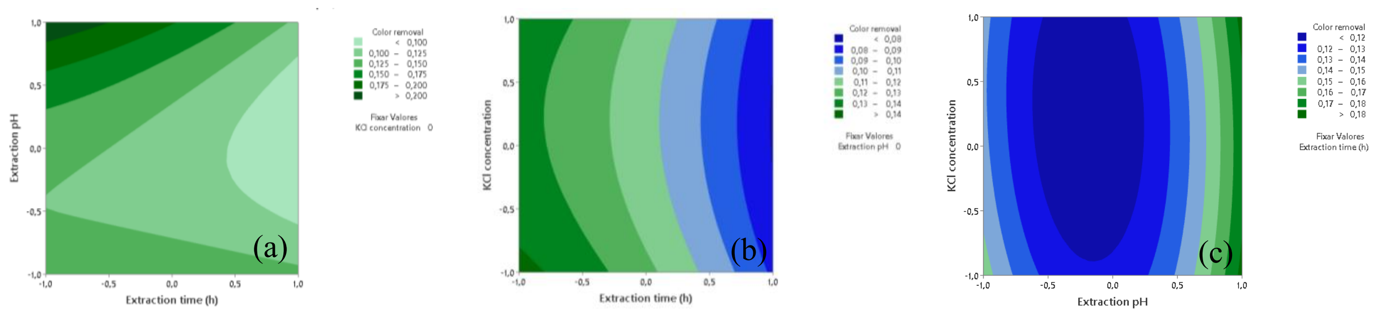

Figure 31. Contour plots for color removal efficiency using eucalyptus bark biocoagulant (0.5 mL dosage) as a function of: (a) pH vs. time; (b) KCl concentration vs. time; (c) KCl concentration vs. pH.

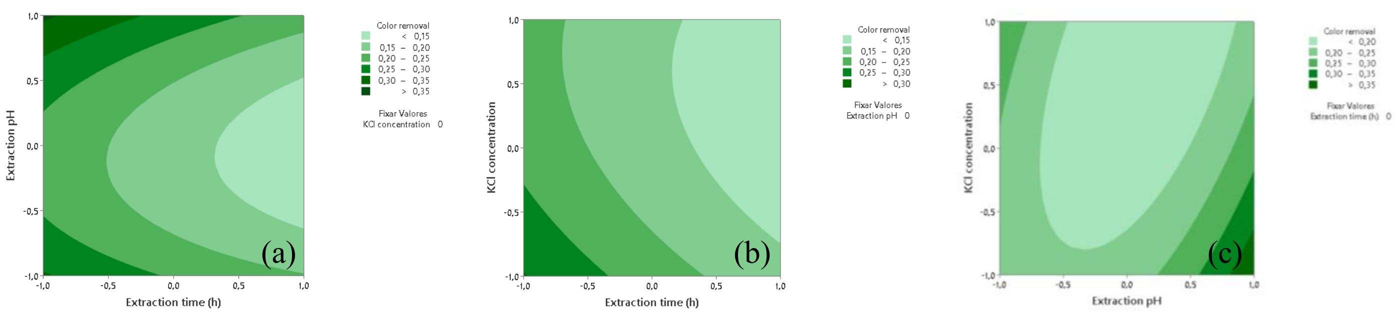

Figure 32. Contour plots for color removal efficiency using eucalyptus bark biocoagulant (1.0 mL dosage) as a function of: (a) pH vs. time; (b) KCl concentration vs. time; (c) KCl concentration vs. pH.

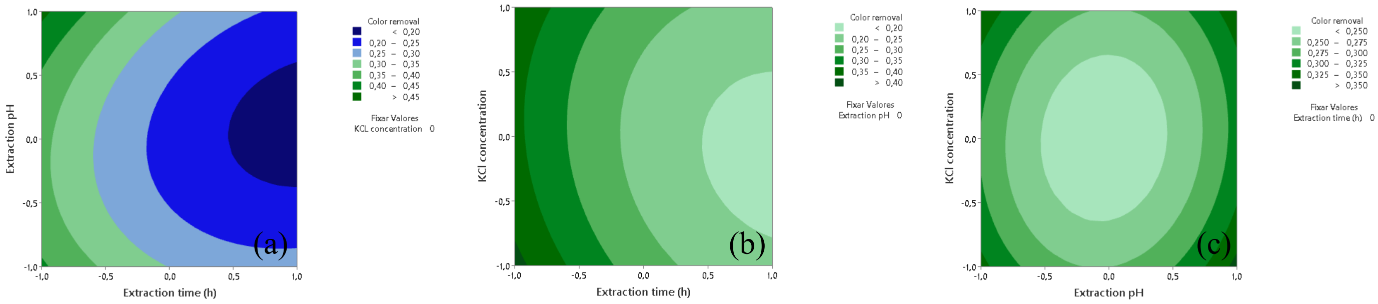

Figure 33. Contour plots for color removal efficiency using eucalyptus bark biocoagulant (1.5 mL dosage) as a function of: (a) pH vs. time; (b) KCl concentration vs. time; (c) KCl concentration vs. pH.

Overall, the color removal efficiency using eucalyptus bark biocoagulant was strongly influenced by the interaction between extraction pH, extraction time, and KCl concentration. However, the response behavior progressively changed according to the applied coagulant dosage, indicating modifications in the relative contribution of the extraction variables to the coagulation performance.

At the lowest dosage (Figure 31), broader and more heterogeneous optimal response regions were observed, indicating a greater sensitivity of color removal efficiency to variations in extraction conditions. The highest color removal efficiencies (>0.20) were generally associated with alkaline extraction conditions (pH 7), short extraction times (12 h), and low KCl concentrations (0.5 M) for all the samples. The contour plots also exhibited dual-response regions in the KCl–pH interaction surface, where high color removal efficiencies were achieved under alkaline conditions combined with both low and high KCl concentrations.

At the intermediate dosage (Figure 32), the contour plots became more concentrated and exhibited stronger nonlinear interaction effects between the evaluated variables. The highest color removal efficiencies (>0.35) were observed under short extraction times (12 h), particularly under strongly acidic (pH 5) and strongly alkaline (pH 7) conditions. The contour plots also demonstrated that low KCl concentrations (0.5 M) were strongly associated with high color removal efficiencies, reinforcing the synergistic interaction between reduced ionic strength and short extraction periods. Compared with the 0.5 mL dosage, the optimal regions became more localized and asymmetric, suggesting a highly interactive system response in which the effect of extraction pH became increasingly dependent on the KCl concentration.

At the highest dosage (Figure 33), the response regions became more homogeneous and stable, whereas the optimal operational conditions remained predominantly associated with alkaline extraction pH (pH 7), short extraction times (12 h), and low KCl concentrations (0.5 M). The highest color removal efficiencies (>0.45) were consistently achieved under these conditions, indicating that reduced ionic strength and mild alkaline extraction strongly favored the preservation and activity of the functional compounds responsible for color removal. Compared with the lower dosages, the contour plots exhibited smoother transitions and broader stable regions, indicating the reduced sensitivity of the system to moderate variations in the operational conditions. The progressive concentration of optimal regions under low ionic strength conditions suggests that an elevated coagulant dosage enhances the effectiveness of adsorption-related removal mechanisms.

The contour plots indicate that color removal using eucalyptus bark biocoagulants is strongly favored under alkaline extraction conditions, short extraction times, and low KCl concentrations. According to Yin (2010), salt-assisted extraction may alter the solubility and dissociation of bioactive compounds through salting-in effects, directly influencing the extraction efficiency of active substances under different ionic strengths. Anastopoulos et al. (2022) reported that eucalyptus-based adsorbents exhibit high affinity toward dye molecules due to the presence of functional groups capable of promoting electrostatic attraction, hydrogen bonding, pore filling, and surface adsorption interactions. In addition, the adsorption efficiency of eucalyptus-derived materials is strongly influenced by pH, ionic strength, and contact time, which directly affect the availability and activity of adsorption sites. Similar adsorption-related behaviors have also been reported for plant-based coagulants rich in proteins and polysaccharides, whose functional groups may contribute to color removal through surface adsorption and molecular interactions, which are strongly influenced by extraction conditions and solution chemistry (Choy et al., 2014). These mechanisms may explain the progressive stabilization of the response surfaces and the strong influence of KCl concentration observed across the evaluated eucalyptus bark biocoagulant dosages.

To better visualize the experimental trends identified in the contour plots, complementary experimental trend plots based on the observed color removal efficiencies were constructed (Figures 34, 35, and 36). These plots provide a direct representation of the influence of extraction time, extraction pH, and KCl concentration on color removal performance at different eucalyptus bark biocoagulant dosages. The graphs were generated using the average removal efficiencies obtained at each evaluated operational level, allowing a clearer interpretation of the dominant experimental trends while maintaining the multivariable characteristics of the Box–Behnken design.

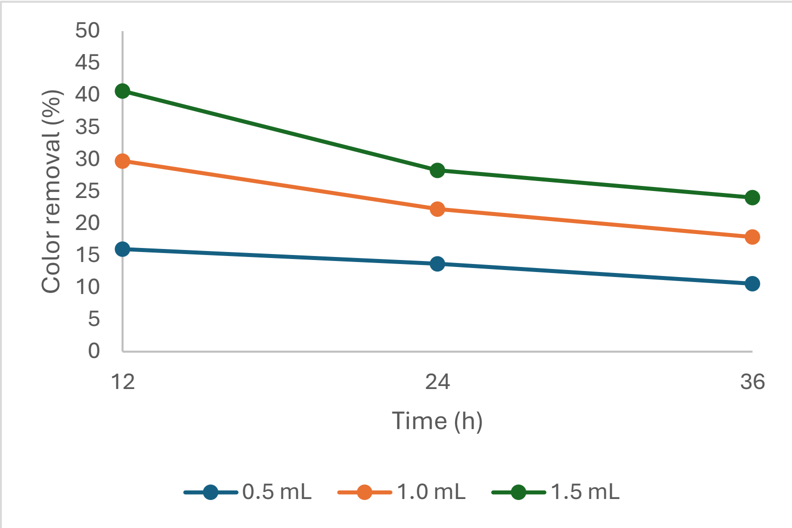

Figure 34. Effect of extraction time on color removal.

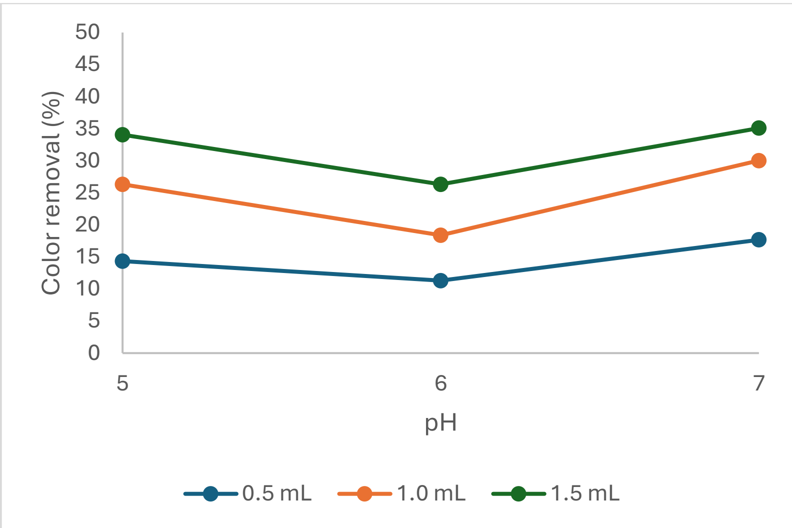

Figure 35. Effect of extraction pH on color removal.

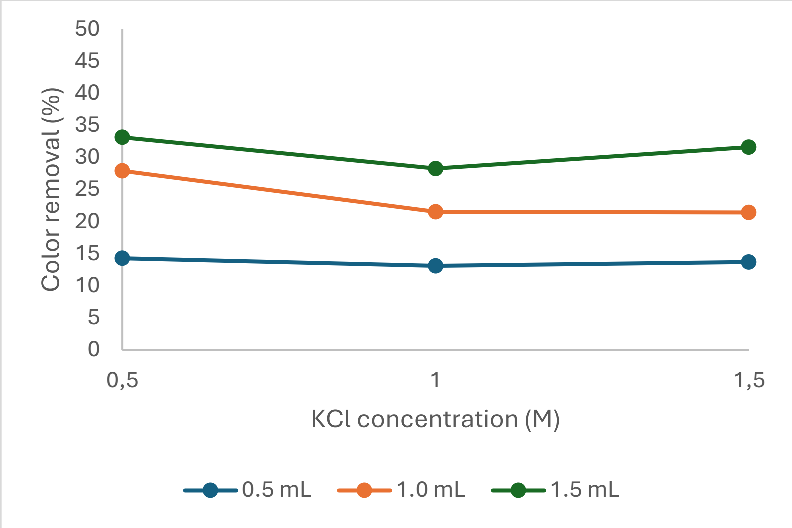

Figure 36. Effect of KCl concentration on color removal.

Overall, the experimental trend plots strongly corroborated the tendencies previously identified in the contour plots, reinforcing the consistency of the operational behavior observed across the evaluated eucalyptus bark biocoagulant dosages. Both graphical approaches consistently demonstrated that short extraction times favored color removal efficiency. Similarly, for the 1.0 and 1.5 mL dosages, both the contour and experimental trend plots indicated that alkaline extraction conditions and low KCl concentrations generally promoted higher color removal efficiencies.

Specifically, the contour plots in Figure 31 suggested that neutral pH, short extraction times, and low KCl concentrations favored color removal at the lowest dosage, as observed in Figures 34–36.

At the intermediate dosage, the contour plots in Figure 32 demonstrated localized optimal regions associated with short extraction times under both acidic and alkaline extraction conditions, which is also reflected in Figure 35. In addition, the stronger influence of the low KCl concentration identified in the contour analysis is directly corroborated by Figure 36.

At the highest dosage, both graphical approaches consistently indicated progressive stabilization of the coagulation system. The contour plots in Figure 33 suggested that neutral extraction conditions, short extraction times, and low KCl concentrations remained the main favorable operational conditions, as confirmed by Figures 34–36.

4.4 Comparative Analysis Between Walnut Shell and Eucalyptus Bark

The comparative analysis between walnut shell and eucalyptus bark biocoagulants revealed important differences in both the experimental performance and statistical behavior of the fitted models. Although walnut shells achieved competitive turbidity removal under specific operational conditions, eucalyptus bark generally presented higher removal efficiencies, greater statistical consistency, and better model predictability, particularly for color removal.

Regarding turbidity removal, walnut shells exhibited moderate experimental performance, with maximum removal efficiencies close to 80% under specific operational conditions (24 h, pH 8, 0.5 M NaCl), although there was considerable variability throughout the experimental domain. This instability is reflected in the ANOVA results, in which all turbidity models for walnut shells were statistically non-significant for the evaluated dosages (with the best p-value > 0.43), accompanied by relatively low coefficients of determination (R^2 between 41% and 60%) and adjusted R^2 values close to zero.

For color removal, the walnut shells showed a greater dependence on specific operational conditions and lower statistical stability. At 0.5 mL and 1.5 mL, the model was not significant, and only at 1.0 mL, the model became statistically significant ($p = 0.030$), with $R^2 = 85.24\%$ and adjusted $R^2 = 66.27\%$, in which the main effects were associated with the pH × NaCl interaction ($p = 0.004$) and $NaCl^2$ ($p = 0.036$).

For eucalyptus bark, turbidity removal exhibited generally superior experimental performance, reaching values of up to 90% at a 0.5 mL dosage (36 h, pH 5, 1.0 M KCl). From the statistical perspective of the ANOVA analysis, the 1.0 mL dosage showed the best predictive capability with $R^2 = 80.85\%$, although with $p = 0.066$, but with good specific factors in extraction time ($p = 0.006$) and pH^2 ($p = 0.012$). At the 1.5 mL dosage, the model maintained relatively good predictive performance with $R^2 = 76.07\%$, even with $p = 0.123$, and with significant effects, particularly for extraction time ($p = 0.016$) and pH^2 ($p = 0.021$).

With respect to color removal, eucalyptus bark clearly outperformed walnut shell in terms of removal percentage and statistical analysis. Experimentally, eucalyptus bark achieved color removal efficiencies above 40 under several operational conditions, whereas the walnut shell only reached similar values under one specific condition. Good results were obtained in the overall analysis and at some specific points for 1.0 mL ($p = 0.016$, $R^2 = 87.98\%$, and adjusted $R^2 = 72.51$), and the best results were obtained at 1.5 mL ($p = 0.006$, $R^2 = 91.27\%$, and adjusted $R^2 = 80.05\%$). In this case, the extraction time ($p < 0.001$) and pH^2 ($p = 0.006$) were highly significant variables.

Overall, eucalyptus bark demonstrated superior coagulation performance, greater statistical consistency, and better model predictability, particularly for color removal at higher dosage levels. The recurring significance of extraction time and pH^2 indicates a more stable and mechanistically coherent behavior, likely associated with tannins, lignocellulosic compounds, and active functional groups capable of promoting coagulation–flocculation and adsorption mechanisms (Khelladi et al., 2026; Anastopoulos et al., 2022). In contrast, walnut shells showed competitive turbidity removal under specific operational conditions but exhibited greater variability and lower statistical robustness, especially for turbidity models. This behavior is consistent with reports for lignocellulosic natural coagulants, whose performance strongly depends on extraction conditions, ionic strength, and the availability of active polymeric compounds (Choy et al., 2014). These results suggest that eucalyptus bark has greater potential for stable and reproducible coagulation performance, whereas walnut shells may require narrower optimization conditions to achieve comparable treatment efficiencies.

Studies related to turbidity and color removal under different experimental conditions were selected for comparison with the results obtained in the present study. In general, the turbidity results reported in the literature showed behavior similar to that observed in this study, whereas more pronounced differences were observed for color removal. These differences may be mainly attributed to the distinct methodologies employed by the authors, including the use of solid biomass, liquid extracts obtained through aqueous extraction, and adsorption-based systems, unlike the present study, in which a saline-assisted liquid extraction strategy was used. The selected studies are presented in a generalized manner in Tables 9 and 10.

Table 9. Comparative studies on turbidity removal for different types of residues.

Reference	Biomass Type	Preparation Method	Water / Matrix Type	Turbidity Removal (%)
Semassel et al. (2025)	Walnut shell	Shelled, rinsed, dried (100 °C/10 h), crushed, sieved. Stock: 50 g L^{-1}.	Landfill leachate	83.9 at pH 4.0, 75.5 at pH 6.0 and 61.31 at pH 8.0.
	Moringa oleifera seed	Shelled, dried (50 °C/24 h), ground, sieved. Stock: 50 g L^{-1}.		91.85 at pH 5.0; 83.63 at pH 6.0; 77.14 at pH 8.0.
	Opuntia ficus-indica leaf	Cleaned, spines removed, sliced, dried (40 °C/3 h → 80 °C), ground. Stock: 50 g L^{-1}.		86.0 at pH 6.0 and 36.47 at pH 8.0.
Siddique et al. (2016)	Walnut shell	Washed with distilled water, dried (24 °C), ground, sieved.	Synthetic kaolin-based turbid water	83.0 for 35 mg L^{-1} dosage
Shahzadi et al. (2024)	Sorghum seed powder	Dried (48 h sunlight → 103 °C/24 h), blended, sieved	Surface water	89.2
	Aloe vera leaves	Thick exterior removed, pulp blended.		70.8
Zedan et al. (2022)	Walnut pulp (seeds)	Rinsed, dried (room temp/24 h), ground, sieved (0.4 mm). 4 g added to 1,000 mL of 1.0 M NaCl.	Synthetic kaolin water	99.5 at 20 mg L^{-1} dosage
Uwanta et al. (2022)	Eucalyptus bark	Air-dried, ground, sieved (0.8 mm). tested directly as fine powder.	Pond water	50
Khelladi et al. (2026)	Agave	Rinsed, oven-dried (105 °C and 60–90 °C/72 h), processed, sieved. Extract: 1 g L^{-1}	Domestic wastewater	97.76 at 20 mg L^{-1} dosage.
	Eucalyptus leaves			88.05 at 90 mg L^{-1} dosage

Table 10. Comparative studies on color removal for different types of residues.

Reference	Biomass Type	Target Pollutant / Dye	Extraction / Preparation Parameters	Color Removal (%)
Zourif et al. (2024)	Walnut husks	Methylene blue	Ground walnut husks with optimized particle size.	89.48
Semassel et al. (2025)	Walnut shell	Leachate (pH: 8.3, Turbidity: 400 NTU)	Shelled, rinsed, dried (100 °C/10 h), crushed, sieved. Stock: 50 g L^{-1} in demineralized water.	60.0
	Moringa oleifera seed		Shelled, dried (50°C/24 h), ground, sieved. Stock: 50 g L^{-1}.	76.25
	Opuntia ficus-indica leaf		Cleaned, spines removed, sliced, dried (40 °C/3 h → 80 °C), ground. Stock: 50 g L^{-1}.	60.15
Sivalingam et al. (2023)	Moringa oleifera	Magenta Dye	Seeds were ground and subjected to NaCl and KCl extraction solutions.	93.0
Hadadi et al. (2022)	Moringa oleifera	Mordant Black 11 (Azo dye)	Seeds were dried at 40 °C for 24h then were submitted to aqueous extraction.	80.12
El Gaayda et. al. (2022)	Moringa oleifera seed	Amido Black 10B dye	Oven-dried (50 °C/24 h), ground.	92.2

5. Economic Feasibility Analysis of Lignocellulosic Biocoagulants

5.1 Economic Assessment of Biocoagulant Production

To provide a more realistic preliminary economic assessment for industrial applications, the production costs of the developed biocoagulants were re-estimated using commercially available sodium chloride and potassium chloride products instead of analytical-grade laboratory reagents. Commercial sea salt commonly used for food applications was considered as the NaCl source (0.29 €/kg), whereas commercially available potassium chloride-based low-sodium salt substitutes were considered as KCl sources (11 €/kg).

As walnut shells and eucalyptus bark are agro-industrial and forestry residues, respectively, no direct raw material acquisition costs were considered for the biomasses themselves, reinforcing the low-cost and waste valorization potential of the proposed approach. Water costs, without considering equipment costs, were estimated based on industrial reverse osmosis production values reported by Feo-García et al. (2024), considering that for average water production capacities between 15,000 and 60,000 m^3/day, the average production cost is approximately 0.60 EUR/m^3.

To evaluate the potential applicability of the developed biocoagulants under large-scale operating conditions, a simplified simulation for the treatment of 1 m^3 of water was performed based on the average experimental dosage adopted during the jar test assay. Considering that approximately 1 mL of biocoagulant extract was required to treat 100 mL of water, the extract-to-water volumetric ratio corresponded to approximately 10 L of biocoagulant extract per cubic meter of treated water. Based on this proportion, the estimated extraction-stage production costs associated with 1 m^3 of water treatment were calculated and are presented in Tables 11 and 12.

Table 11. Estimated production cost of walnut shell biocoagulant extract (per 10 L).

NaCl (M)	NaCl required (Kg)	NaCl cost (€)	Water cost (€)	Total cost (€ / 10 L extract)
0.5	2.92	0.85	0.006	0.86
1.0	5.84	1.69	0.006	1.70
1.5	8.77	2.54	0.006	2.55

Table 12. Estimated production cost of eucalyptus bark biocoagulant extracts (per 10 L).

KCl concentration	KCl required (Kg)	KCl cost (€)	Water cost (€)	Total cost (€ / 10 L extract)
0.5 M	3.73	41.03	0.006	41.04
1.0 M	7.46	82.06	0.006	82.07
1.5 M	11.18	122.98	0.006	122.99

The results indicate that NaCl-assisted extraction is considerably more economically competitive because of the low commercial cost and wide availability of sodium chloride-based products. In contrast, KCl-assisted extraction resulted in significantly higher estimated production costs, despite the superior coagulation performance and greater statistical consistency observed in eucalyptus bark extracts.

Nevertheless, these findings reinforce the potential applicability of saline-assisted natural biocoagulant extraction systems as low-cost and environmentally friendly alternatives for water treatment. Furthermore, the proposed approach contributes to green economy principles through the valorization of agro-industrial and forestry residues, reducing dependence on conventional chemical coagulants, and promoting the development of more sustainable treatment strategies with lower environmental impact.

6. Conclusions

Concerns over water resource management and the need for sustainable wastewater treatment alternatives have driven this research. This study explored the potential of biocoagulants derived from walnut shells (Juglans regia) and eucalyptus bark (Eucalyptus spp.) as ecological substitutes for conventional chemical coagulants. The adopted approach, distinguished by the use of saline-assisted liquid extracts, represents a milder and more environmentally aligned extraction route, avoiding the need for raw powders or chemically activated adsorbents often reported in the literature.

The results obtained demonstrate the differentiated effectiveness of the tested biocoagulants. Eucalyptus bark stood out in turbidity removal, achieving a remarkable efficiency of 90% under acidic and saline conditions, surpassing walnut shells, which reached approximately 80% removal under optimized NaCl-assisted extraction conditions. This superiority of eucalyptus bark, accompanied by greater statistical consistency, underscores its promising role in water clarification.

Regarding color removal, using methylene blue as a model dye, both biomaterials exhibited comparable performances, with efficiencies of approximately 47% for both walnut shells and eucalyptus bark. Although these efficiencies are lower than those observed in chemically activated or highly optimized systems in the literature, the relevance of our findings lies in the sustainability and simplicity of the process. The absence of chemical activation procedures and the use of mild extraction strategies provide these biocoagulants with low environmental impact and operational ease, making them viable and low-cost alternatives.

In summary, this research validates an innovative extraction strategy that allows the conversion of agro-industrial and forestry lignocellulosic residues into functional biocoagulants through simple and sustainable processing routes. These findings reinforce the potential applicability of saline-assisted natural biocoagulant systems as environmentally friendly alternatives for preliminary water clarification and partial dye removal in wastewater treatment. This work not only contributes to the advancement of sustainable water treatment technologies but also promotes waste valorization, aligning with the objectives of a circular economy and a greener future for water resource management.

References

Abdo, S. M., Mahmoud, R. H., Youssef, M., El-Naggar, M. E. (2020). Cationic starch and polyaluminum chloride as coagulants for River Nile water treatment. Groundwater for Sustainable Development, 10, 100331. https://doi.org/10.1016/j.gsd.2020.100331

Acoglu Celik, B., Celik, M. A., Jūrienė, L., Jovaišaitė, J., Kazernavičiūtė, R., Bekar, E., Yolci Omeroglu, P., Venskutonis, P. R., Kamiloglu, S. (2025). Biorefining of walnut shells into polyphenol-rich extracts using ultrasound-assisted, enzyme-assisted, and pressurized liquid extraction coupled with chemometrics. Foods, 14(13), 2245. https://doi.org/10.3390/foods14132245

Al-Hanaktah, A., Pérez, S. M. (2026). Natural coagulants extracted from leaf, shell, and kernel of Jatropha curcas for turbidity treatment. Applied Science and Engineering Progress, 19(1), 7847. https://doi.org/10.14416/j.asep.2025.08.003

Anastopoulos, I., Ahmed, M. J., Hummadi, E. H. (2022). Eucalyptus-based materials as adsorbents for heavy metals and dyes removal from (waste)waters. Journal of Molecular Liquids, 356, 118864. https://doi.org/10.1016/j.molliq.2022.118864

Benalia, A., Derbal, K., Amrouci, Z., Baatache, O., Khalfaoui, A., Pizzi, A. (2024). Application of plant-based coagulants and their mechanisms in water treatment: A review. Journal of Renewable Materials, 12(4), 675–702. https://doi.org/10.32604/jrm.2024.048306

Carneiro, P. A., Umbuzeiro, G. A., Oliveira, D. P., Zanoni, M. V. B. (2010). Assessment of water contamination caused by a mutagenic textile effluent/dyehouse effluent bearing disperse dyes. Journal of Hazardous Materials, 174(1–3), 694–699. https://doi.org/10.1016/j.jhazmat.2009.09.106

Celeiro. (n.d.). *LoSalt: Sal com teor de sódio reduzido*. Celeiro Online. Retrieved May 27, 2026, from https://www.celeiro.pt/9997-sal-com-teor-de-sodio-reduzido-350-gramas-kg-losalt

Chemetova, C., Fabião, A., Gominho, J., Ribeiro, H. (2018). Range analysis of Eucalyptus globulus bark low-temperature hydrothermal treatment to produce a new component for growing media industry. Waste Management, 79, 1–7. https://doi.org/10.1016/j.wasman.2018.07.019

Choy, S. Y., Prasad, K. M. N., Wu, T. Y., Raghunandan, M. E., Ramanan, R. N. (2014). Utilization of plant-based natural coagulants as future alternatives towards sustainable water clarification. Journal of Environmental Sciences, 26(11), 2178–2189. https://doi.org/10.1016/j.jes.2014.09.024

Continente. (n.d.). *Sal grosso Continente*. Continente Online. Retrieved May 27, 2026, from https://www.continente.pt/produto/sal-grosso-continente-continente-5621031.html

El Gaayda, J., Titchou, F. E., Barra, I., Karmal, I., Afanga, H., Zazou, H., Yap, P.-S., Abidin, Z. Z., Hamdani, M., Ait Akbour, R. (2022). Optimization of turbidity and dye removal from synthetic wastewater using response surface methodology: Effectiveness of Moringa oleifera seed powder as a green coagulant. Journal of

Environmental Chemical Engineering, 10(1), 106988. https://doi.org/10.1016/j.jece.2021.106988

Feo-García, J., Pulido-Alonso, A., Florido-Betancor, A., & Florido-Suárez, N. R. (2024). Cost Studies of Reverse Osmosis Desalination Plants in the Range of 23,000–33,000 m^3/day. *Water*, *16*(6), 910. https://doi.org/10.3390/w16060910

Food and Agriculture Organization of the United Nations. (2020). Global forest resources assessment 2020: Main report. FAO. https://doi.org/10.4060/ca9825en

Geissdoerfer, M., Savaget, P., Bocken, N. M. P., Hultink, E. J. (2017). The circular economy – A new sustainability paradigm? Journal of Cleaner Production, 143, 757–768. https://doi.org/10.1016/j.jclepro.2016.12.048

Grenda, K., Gamelas, J. A. F., Arnold, J., Cayrec, O. J., Rasteiro, M. G. (2019). Cationization of eucalyptus wood waste pulps with diverse lignin contents for potential application in colored wastewater treatment. RSC Advances, 9(60), 34857–34869. https://doi.org/10.1039/C9RA05757A

Grenda, K., Gamelas, J. A. F., Arnold, J., Pellizzer, L., Cayre, O. J., Rasteiro, M. G. (2021). Evaluation of anionic eco-friendly flocculants prepared from eucalyptus pulps with diverse lignin contents for application in effluent treatment. Polymers, 13(1), 25. https://doi.org/10.3390/polym13010025

Hadadi, A., Imessaoudene, A., Bollinger, J.-C., Cheikh, S., Assadi, A. A., Amrane, A., Kebir, M., Mouni, L. (2022). Parametrical study for the effective removal of Mordant Black 11 from synthetic solutions: Moringa oleifera seeds' extracts versus alum. Water, 14(24), 4109. https://doi.org/10.3390/w14244109

Husen, A. K., Bidira, F., Desta, W. M., Asaithambi, P. (2024). COD, color, and turbidity reduction from surface water using natural coagulants: Investigation and optimization. Progress in Engineering Science, 1(2–3), 100007. https://doi.org/10.1016/j.pes.2024.100007

Jahanban-Esfahlan, A., Jahanban-Esfahlan, R., Tabibiazar, M., Roufegarinejad, L., Amarowicz, R. (2020). Recent advances in the use of walnut (Juglans regia L.) shell as a valuable plant-based bio-sorbent for the removal of hazardous materials. RSC Advances, 10(12), 7026–7047. https://doi.org/10.1039/C9RA10084A

Khan, N. A., López-Maldonado, E. A., Majumder, A., Singh, S., Varshney, R., López, J. R., Méndez, P. F., Ramamurthy, P. C., Khan, M. A., Khan, A. H., Mubarak, N. M., Ahmad, W., Shamshuddin, S. Z. M., Aljundi, I. H. (2023). A state-of-art-review on emerging contaminants: Environmental chemistry, health effect, and modern treatment methods. Chemosphere, 344, 140264. https://doi.org/10.1016/j.chemosphere.2023.140264

Khelladi, R. M. B., Chiboub Fellah, A., Benyagoub, M., Chiboub Fellah, F. Z., Rahmani, Z., Benadda, L. (2026). Enhanced coagulation-flocculation of domestic wastewater using sustainable plant-based material: A comparative study of nopal, agave, and eucalyptus. Water SA, 52(2), 151–160. https://doi.org/10.17159/wsa/2026.v52.i2.4247

Kirchherr, J., Reike, D., Hekkert, M. (2017). Conceptualizing the circular economy: An analysis of 114 definitions. Resources, Conservation and Recycling, 127, 221–232. https://doi.org/10.1016/j.resconrec.2017.09.005

Klumb, A. K., Faria, O. L. V. (2013). Produção de coagulante vegetal catiônico a partir de cascas de Eucalipto (Eucalyptus tereticornis). VETOR - Revista de Ciências Exatas e Engenharias, 22(1), 71–80. https://periodicos.furg.br/vetor/article/view/2009

Lim, H. R., Choo, C. M., Chong, C. H., Wong, V.-L. (2021). Optimization studies for water defluoridation with two-stage coagulation processes using new industrial-based chemical coagulants. Journal of Water Process Engineering, 42, 102179. https://doi.org/10.1016/j.jwpe.2021.102179

Lima, P. R., Almeida, I. V., Vicentini, V. E. P. (2020). Os diferentes tipos de coagulantes naturais para o tratamento de água: Uma revisão. Evidência: Biociências, Saúde e Inovação. https://doi.org/10.18593/eba.24704

Menezes, H. C., Orlando, R. M., Augusti, R., Macedo, A. N., Almeida, M. R., Cardeal, Z. L., Valenzuela, E. F., Ribeiro, C. C., Avelar, M. C. F., Freitas, M. C. de, Silva, L. P. da, Gomes, J. M., Gomes, J. C. L., Augusti, J. V., Lopes, B. O., Melo, N. de O., Silva, L. P. M. da, Sousa, D. V. M. de. (2025). Analysis of contaminants in surface water after the collapse of the Córrego do Feijão mine dam in Brumadinho, Brazil. Science of The Total Environment, 990, 179954. https://doi.org/10.1016/j.scitotenv.2025.179954

Miranda, I., Gominho, J., Mirra, I., Pereira, H. (2013). Fractioning and chemical characterization of barks of Betula pendula and Eucalyptus globulus. Industrial Crops and Products, 41, 299–305. https://doi.org/10.1016/j.indcrop.2012.04.024

Mohammad Ali, N. F. H., Megat Hanafiah, M. A. K., Saleh, S. H., Mohd Ali, M. T., Ibrahim, S. (2024). A review of biomass-based natural coagulants for water pollution remediation: Impact of properties and coagulation operational parameters. AUIQ Complementary Biological System, 1(2), Article 4. https://doi.org/10.70176/3007-973X.1013

Ndayako, A., Sani, B., Abubakar, U., Isama, S., Yakubu, A. (2023). Assessing the efficacy of bio-coagulants in water treatment. European Journal of Applied Science, Engineering and Technology, 1(1), 20–29. https://doi.org/10.59324/ejaset.2023.1(1).03

Nujkic, M., Milić, S., Papludis, A., Stanković, S., Radojevic, A., Alagić, S., Spalović, B. (2020). Walnut shell as a biosorbent for removal of heavy metal ions from different sample solutions.

Semassel, S. E., Elhadeuf, K., Bougdah, N., Messikh, N. (2025). Enhancing the clarification of Azzaba landfill leachate using biocoagulants with optimization by Box–Behnken design. Chemistry Chemical Technology, 19(2), 307–326. https://doi.org/10.23939/chcht19.02.307

Shahzadi, F., Haydar, S., Tabraiz, S. (2024). Optimization of coagulation to remove turbidity from surface water using novel nature-based plant coagulant and response surface methodology. Sustainability, 16(7), 2941. https://doi.org/10.3390/su16072941

Siddique, M., Soomro, S., Jatoi, A., Unar, I. (2016). Removal of turbidity from turbid water by bio-coagulant prepared from walnut shell.

Simões, C. L., Santos Neto, A. B. P., Rodrigues, A. C., Ferreira, R., Simoes, R. (2025). Environmental assessment of tannin extraction from bark residues for application in water treatment. Biomass, 5(1), 15. https://doi.org/10.3390/biomass5010015

Sivalingam, S., Vijayaraghavan, G., Vimalkumar, A. (2023). Efficient removal of magenta dye from water by both natural and chemical coagulants. RASAYAN Journal of Chemistry, 16, 307–311. https://doi.org/10.31788/RJC.2023.1618115

Tomasi, I. T., Santos, S. C. R., Boaventura, R. A. R., Botelho, C. M. S. (2023). Microwave-assisted extraction of polyphenols from eucalyptus bark—A first step for a green production of tannin-based coagulants. Water, 15(2), 317. https://doi.org/10.3390/w15020317

Uwanta, E. J., Nicholas, E.-O. S., Ukoha, P. O., Agala, C. T. (2022). Evaluation of the phytochemical properties of Eucalyptus citriodora exudates and its potency as coagulant in water purification. Chemistry and Materials Research, 14(4). https://doi.org/10.7176/CMR/14-4-03

Vilela, C. L. S., Bassin, J. P., Peixoto, R. S. (2018). Water contamination by endocrine disruptors: Impacts, microbiological aspects and trends for environmental protection. Environmental Pollution, 235, 546–559. https://doi.org/10.1016/j.envpol.2017.12.098

World Population Review. (2026). Walnut production by country. https://worldpopulationreview.com/country-rankings/walnut-production-by-country

Yin, C.-Y. (2010). Emerging usage of plant-based coagulants for water and wastewater treatment. Process Biochemistry, 45(9), 1437–1444. https://doi.org/10.1016/j.procbio.2010.05.030

Zedan, T., Mossad, M., Fouad, M., Mahanna, H. (2022). Potential application of natural coagulant extraction from walnut seeds for water turbidity removal. Water Practice Technology, 17, 684–698. https://doi.org/10.2166/wpt.2022.019

Zourif, A., Benbiyi, A., Kouniba, S., El Guendouzi, M. (2024). Valorization of walnut husks as a natural coagulant for optimized water decolorization. Arabian Journal of Chemistry, 17, 105399. https://doi.org/10.1016/j.arabjc.2023.105399